Aus dem Experimental and Clinical Research Center (ECRC) und der
Medizinischen Klinik m.S. Nephrologie und Internistische Intensivmedizin
der Medizinischen Fakultät Charité – Universitätsmedizin Berlin

DISSERTATION

TRPC6 in Renal Fibrosis and Immune Cell Infiltration after Unilateral Ureteral Obstruction

zur Erlangung des akademischen Grades
Doctor medicinae (Dr. med.)

vorgelegt der Medizinischen Fakultät
Charité – Universitätsmedizin Berlin

von

Weiying Kong

aus Shanghai, China

Datum der Promotion: 06.03.2020

meinen Eltern gewidmet

TABLE OF CONTENTS / INHALTSVERZEICHNIS

List of figures and tables / Abbildungs- und Tabellenverzeichnis

Abbreviations / Abkürzungsverzeichnis

αSMA	alpha smooth muscle actin
ACEI	angiotensin-converting enzyme inhibitors
AKI	acute kidney injury
Ang II	angiotension II
ARB	angiotensin II receptor blockers
cCasp3	cleaved-caspase 3
CD2AP	CD2-associated protein
CKD	chronic kidney disease
Col1α1	collagen type 1 alpha 1
Col3α1	collagen type 3 alpha 1
Col4α1	collagen type 4 alpha 1
CVD	cardiovascular disease
DAB	3,3’-diaminobenzidine
eEF1α1	eukaryotic translation elongation factor 1 alpha 1
EGFR	epidermal growth factor receptor
EMT	epithelial-to-mesenchymal transition
ESRD	end-stage renal disease
FMT	fibroblast-to-myofibroblast transdifferentiation
FSGS	focal segmental glomerulosclerosis
GAPDH	glyceraldehyde-3-phosphate dehydrogenase
GBD	global burden of disease
GFR	glomerular filtration rate
ICAM1	intercellular adhesion molecule 1
IHC	immunohistochemistry
IL1β	interleukin 1 beta
IL6	interleukin 6
MBD	mineral and bone disorder
MCP1	monocyte chemotactic protein 1
NSAIDs	non-steroidal anti-inflammatory drugs
NZO	New Zealand Obese

PAS	Periodic acid Schiff
PBS	phosphate-buffered saline
PCNA	proliferating cell nuclear antigen
PECs	parietal epithelial cells
PFA	paraformaldehyde
PGA	polyglycolic acid
PPI	proton pump inhibitors
PTH	parathyroid hormone
RAS	renin-angiotensin system
RRT	renal replacement therapies
SPF	specific pathogen free
SR	Sirius red
STZ	streptozotocin
TDs	transmembrane domains
TGFα	transforming growth factor-α
TGFβ1	transforming growth factor beta 1
TNFα	tumor necrosis factor alpha
TRPCs	transient receptor potential cation channels
TRPC6	transient receptor potential cation channel subfamily C member 6
UUO	unilateral ureter obstruction
VCAM1	vascular cell adhesion molecule 1
WT	wide-type

Abstract

Background:

Chronic kidney disease (CKD) has become a heavy burden globally with rising prevalence. Irrespective of the underlying etiology, renal fibrosis occurs in virtually every type of CKD. The transient receptor potential cation channel subfamily C member 6 (TRPC6) is widely expressed in renal tissues and has been implicated in renal fibrosis. The aims of this study were (i) to examine whether deletion of TRPC6 impacts on renal fibrosis and inflammatory cell infiltration in an early CKD model of unilateral ureter obstruction (UUO) in mice and (ii) whether TRPC6-deficiency as well as UUO affect the regulation of TRPC channel expression in murine kidneys.

Materials and Methods:

UUO- and sham-surgeries were performed in 9-12 weeks old male *Trpc6*$^{-/-}$ mice, wild-type (WT) controls and New Zealand obese (NZO) mice. Seven days after surgery, the mice were sacrificed and the kidneys were harvested for further analyses. Renal fibrosis and inflammatory cell infiltration were evaluated by histological and immunohistochemical staining. The mRNA expression of TRPC channels and markers of fibrosis and inflammation in kidney were assessed using real-time quantitative reverse transcription PCR.

Results:

Histological and immunohistochemical analyses revealed less fibrosis and inflammatory cell infiltration in UUO kidneys of *Trpc6*$^{-/-}$ mice compared to UUO kidneys of WT mice. Of note, genomic deletion of TRPC6 also affected the expression of pro-fibrotic genes in UUO *Trpc6*$^{-/-}$ kidneys compared to UUO WT kidneys while the expression of pro-inflammatory genes remained unchanged. Sham and UUO-operated kidneys of WT, *Trpc6*$^{-/-}$ and NZO mice were examined to compare the gene expression of TRPC members. It emerged that UUO caused marked up-regulation of *Trpc6* mRNA in kidneys of WT and NZO mice. These studies also revealed that UUO caused profound changes

in renal expression of multiple other TRPC genes in the presence and absence of TRPC6, which could also have contributed to the renal outcome.

Conclusions:

TRPC6 contributes to renal fibrosis and immune cell infiltration in the UUO mouse model. Therefore, inhibition of TRPC6 emerges as a promising novel therapeutic strategy for treatment of chronic kidney failure in chronic obstructive nephropathy, including in mice carrying susceptibility genes for obesity, diabetes and hypertension. However, confounding genomic and non-genomic effects of other TRPC channels should be taken into consideration to fully comprehend the renoprotective potential of targeting TRPC6 therapeutically under chronic kidney damaging conditions.

Abstrakt

Hintergrund:

Chronische Nierenerkrankung (CKD) ist eine ernst zu nehmende Erkrankung mit weltweit steigender Inzidenz und Prävalenz, die eine Belastung der öffentlichen Gesundheitssysteme geworden ist. Nierenfibrose tritt unabhängig von der zugrunde liegenden Ätiologie bei jeder Art von CKD auf. Der TRPC6-Kanal (für „transient receptor potential cation channel subfamily C member 6“) wird in der Niere umfassend exprimiert und ist an der Pathogenese der Nierenfibrose beteiligt. Die Ziele dieser Arbeit waren (i) zu untersuchen, ob das Ausschalten von TRPC6 auf die Nierenfibrose und die Entzündungszellinfiltration in frühen Stadien der CKD im Mausmodell der unilateralen Ureterobstruktion (UUO) wirkt; und (ii) ob TRPC6-Mangel sowie UUO die Regulation der TRPC-Kanal-Expression in Mäusenieren beeinflussen.

Materialien und Methoden:

UUO- und Schein-Operationen wurden in 9-12 Wochen alten männlichen *Trpc6*$^{-/-}$ Mäusen, Wildtyp (WT) -Kontrollen und NZO (New Zealand obese) Mäusen durchgeführt. 7 Tage nach der Operation wurden die Mäuse getötet und die Nieren für weitere Analysen geerntet. Nierenfibrose und entzündliche Zellinfiltration wurden durch histologische und immunhistochemische Färbungen bewertet. Die mRNA-Expression von TRPC-Kanälen und Markern für Fibrose und Entzündung in der Niere wurde durch die quantitative Reverse-Transkriptase-Echtzeit-PCR bewertet.

Ergebnisse:

Histologische und immunhistochemische Analysen zeigten eine geringere Fibrose und entzündliche Zellinfiltration in UUO-Nieren von *Trpc6*$^{-/-}$ Mäusen im Vergleich zu UUO-Nieren von WT-Mäusen. Bemerkenswerterweise beeinflusste das genomische Ausschalten von TRPC6 auch die Expression der pro-fibrotischen Gene in UUO-*Trpc6*$^{-/-}$ -Nieren im Vergleich zu UUO-WT-Nieren, während die Expression der pro-inflammatorischen Gene unverändert blieb. Schein- und UUO-operierte Nieren von WT-,

Trpc6$^{-/-}$- und NZO-Mäusen wurden auch untersucht, um die Genexpression von TRPC-Mitgliedern zu vergleichen. Es zeigte sich, dass UUO in den Nieren von WT- und NZO-Mäusen eine deutliche Hochregulierung der *Trpc6*-mRNA verursachte. Die Studie hat auch herausgestellt, dass UUO in Anwesenheit oder Abwesenheit von TRPC6-Veränderungen der renalen Expression mehrerer anderen TRPC-Gene verursacht, was zum Nierenergebnis beitragen könnte.

Schlussfolgerungen:

TRPC6 trägt im UUO-Mausmodell, einschließlich bei Mäusen, die die Empfindlichkeitsgene für Fettleibigkeit, Diabetes und Bluthochdruck tragen, zur Nierenfibrose und zur Infiltration von Immunzellen bei. Daher ist die Hemmung von TRPC6 eine vielversprechende neue Therapiestrategie für die Behandlung von chronischem Nierenversagen bei chronisch obstruktiver Nephropathie. Allerdings sollten umfassende genomische und nicht-genomische Wirkungen anderer TRPC-Kanäle berücksichtigt werden, um das renoprotektive Potenzial der therapeutischen Behandlung von TRPC6 unter chronischen Nierenschäden vollständig zu verstehen.

Chapter 1
Introduction

1.1 Facts about chronic kidney disease

1.1.1 Epidemiology

Chronic kidney disease (CKD) is an irreversible change in kidney structure and function caused by a variety of causes. It can last for months or years, and eventually progresses to end-stage renal disease (ESRD). About 10%-15% of the population worldwide is affected by CKD[1]. The Global Burden of Disease (GBD) study estimated that 1.2 million people died from kidney failure in 2015, an increase of 31.7% since 2005[2]. The prevalence of CKD is rising worldwide. CKD has become a heavy burden on public health resources (Figure 1.1)[3].

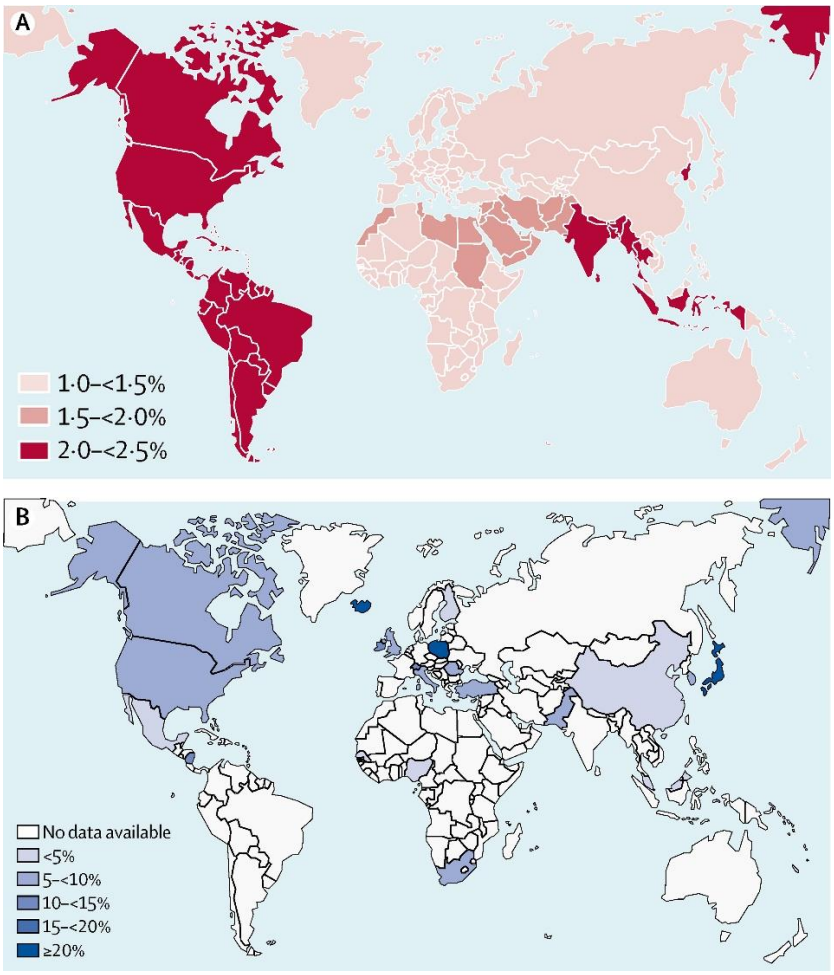

Figure 1.1: **Burden of kidney disease globally.** (A) Proportion of total mortality attributed to kidney disease. (B) Prevalence of chronic kidney disease. *Reprinted from The Lancet, Vol. 389, Webster AC, et al., Chronic Kidney Disease, 1238-1252, Copyright (2017), with permission from Elsevier.* (Ref. 3)

1.1.2 Etiology and pathophysiology

The causes of CKD include diabetic kidney disease, hypertension, vascular disease, glomerular disease (primary or secondary), tubulointerstitial disease, urinary tract obstruction or dysfunction, etc. The leading causes of CKD in high-income, middle-income countries and some low-income countries are diabetes and hypertension [3].

Renal fibrosis is the inevitable consequence of an excessive accumulation of extracellular matrix that occurs in virtually every type of CKD irrespective of the underlying etiology [4]. Renal fibrosis is the principal process underlying the progression of CKD to ESRD. It is characterized by glomerulosclerosis, tubular atrophy, and deposition of excess matrix in the interstitial space surrounding tubules and peritubular capillaries, coupled with the appearance of interstitial fibroblasts[3; 5]. The initiation and progression of renal fibrosis appear to involve a complex, so far incompletely characterized, interaction between injured tubules, pericytes, fibroblasts, endothelial cells and inflammatory cells [5; 6].

Nephron loss is one of the mechanisms of CKD. By activation of the renin-angiotensin system (RAS), transforming growth factor-α (TGFα) and epidermal growth factor receptor (EGFR) as compensatory mechanisms, nephron loss causes compensatory hypertrophy of residual nephrons to maintain the glomerular filtration rate (GFR)[7]. Podocytes also need to undergo hypertrophy to maintain a filtration barrier along the enlarged filtering surface. However, beyond a threshold, the dysfunctional barrier manifests mild proteinuria[7]. In the later stages of CKD, proteinuria and other potential factors inhibit the potential of parietal epithelial cells (PECs) to promote podocyte formation, which in contrast promotes scar formation in the form of focal segmental glomerulosclerosis (FSGS) (Figure 1.2A)[7]. Glomerular hyperfiltration and proteinuria cause an increase in reabsorption of proximal tubules. Albuminuria, complement and immune cells promote the release of proinflammatory mediators in tubular cells, develop interstitial inflammatory response, further FSGS to global glomerulosclerosis, and promote tubular atrophy and interstitial fibrosis. Scar formation is accompanied by vascular reduction and ischemia[7]. Therefore, the residual nephrons need to increase in size to adapt to the high filtration demand, which accelerates the progress of CKD, and creates a vicious circle (Figure 1.2B)[7].

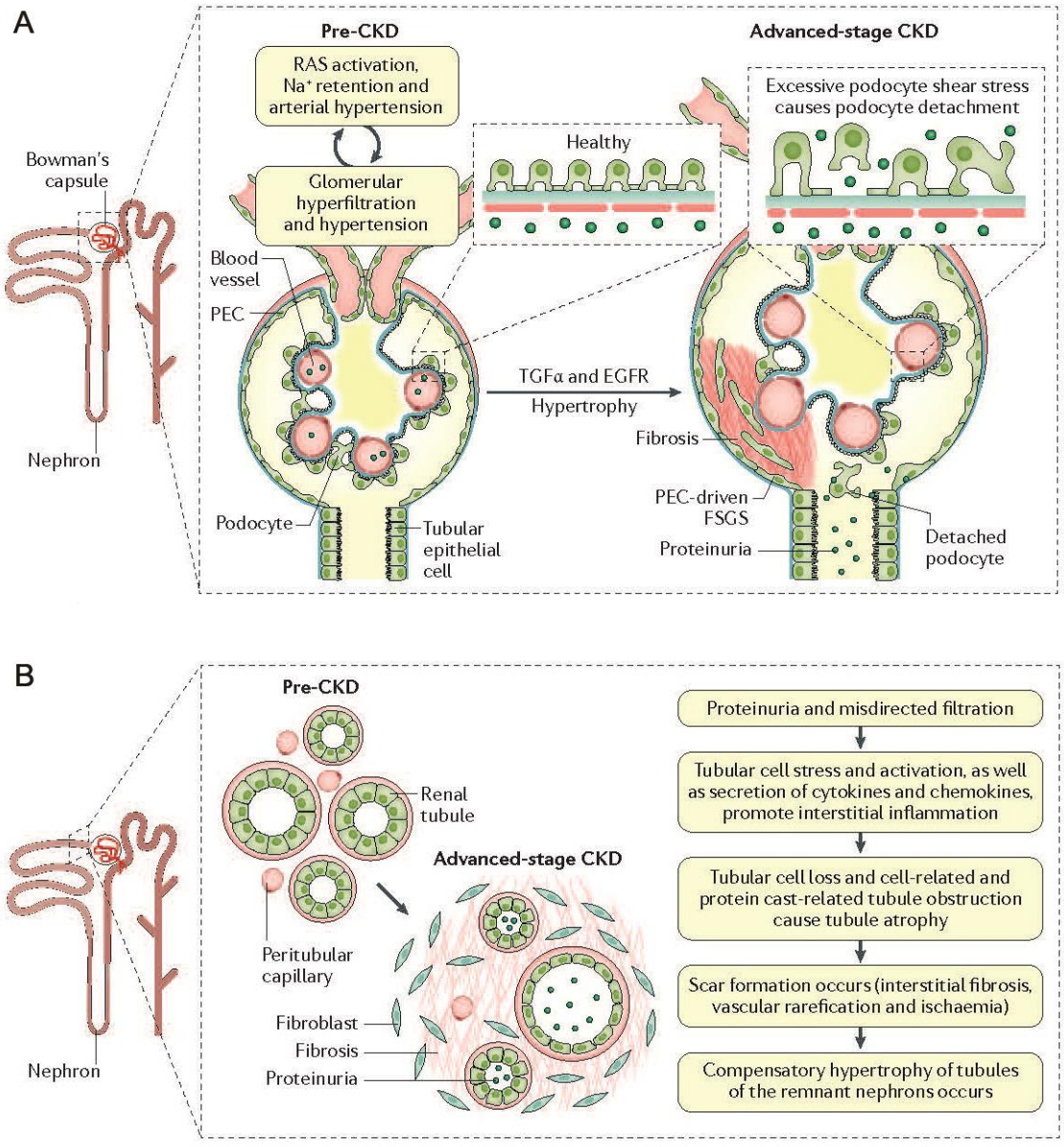

Figure 1.2: **Mechanisms of CKD.** (A) Injury, hyperfiltration and hypertrophy of the nephron. (B) Interstitial fibrosis. *Adapted by permission from Springer Nature: Springer Nature, Nature Reviews Disease Primers, Vol. 3, Romagnani P, et al., Chronic kidney disease, Copyright (2017).* (Ref. 7)

1.1.3 Therapy

There is no cure for CKD, but it is often treatable. The aim of the treatment is to slow or halt the progression of CKD and to prevent serious complications.

In the early stages of CKD, a proper diet and medications are the main treatments. It is important to prevent renal damage and avoid acute kidney injury (AKI) in residual CKD

nephrons. This includes avoiding nephrotoxic drugs (such as high-dose contrast agents, non-steroidal anti-inflammatory drugs (NSAIDs), antibiotics, proton pump inhibitors (PPI), other endemic or occupational toxins), and eliminating hypovolemia and urinary tract obstruction. Reducing dietary salt intake, and controlling blood pressure, blood glucose and blood lipids can further reduce proteinuria and delay CKD progression[7]. Angiotensin-converting enzyme inhibitors (ACEI) and angiotensin II receptor blockers (ARB) are considered the primary medical therapies for delaying the progression to ESRD. Randomized clinical trials have shown that these medications can slow the progression of CKD in individuals with proteinuric (diabetic and nondiabetic) kidney disease[8].

Most people reaching ESRD are treated with renal replacement therapies (RRT), either dialysis (hemodialysis, peritoneal dialysis) or kidney transplantation. A number of secondary complications associated with CKD and ESRD need to be managed. The most relevant complication for all-cause mortality is cardiovascular disease (CVD)[9]. CVD is also associated with endocrine disorders (such as lack of erythropoietin, vitamin D_3 or parathyroid hormone (PTH)) which cause anemia, secondary hyperparathyroidism and mineral and bone disorder (MBD). Ultimately, a variety of factors lead to myocardial fibrosis[10; 11; 12].

In summary, treatment of patients with CKD needs to be considered as follows: controlling further nephron damage, correcting hyperfiltration of individual nephrons, controlling CKD-related complications, and preparing for RRT. The core principle of these treatments is "the sooner, the better" in order to slow the progression to ESRD and to optimize kidney outcomes[7]. Accordingly, considerable efforts are being made to identify novel drug targets to prevent or halt renal fibrosis, the final common pathway of a wide variety of CKD.

1.2 TRPC in the TRP-superfamily

Transient receptor potential (TRP) channels are a non-selective cation channel superfamily with 28 members which are located on the cell membrane based on the structural homology and which show all variations in their Ca^{2+} permeability[13]. The name “transient receptor potential” is based on the discovery of a mutant of *Drosophila*

melanogaster that responds to a light stimulus with a transient rather than a plateau-shaped signal[14; 15]. They are widely expressed in a variety of biological cells and are involved in many physiological processes such as sensory signaling, osmotic pressure regulation, cardiovascular circulation, gastrointestinal motility, airway hyperresponsiveness, anal emptying and cell differentiation processes. The TRP superfamily can be split into several subfamilies: TRPA (ankyrin), TRPC (canonical), TRPM (melastatin), TRPML (mucolipin), TRPN (no mechanoreceptor potential), TRPP (polycystin) and TRPV (vanilloid) [16], and in each subfamily there are many subtypes. All the subfamilies are expressed in humans except TRPN (Figure 1.3)[17].

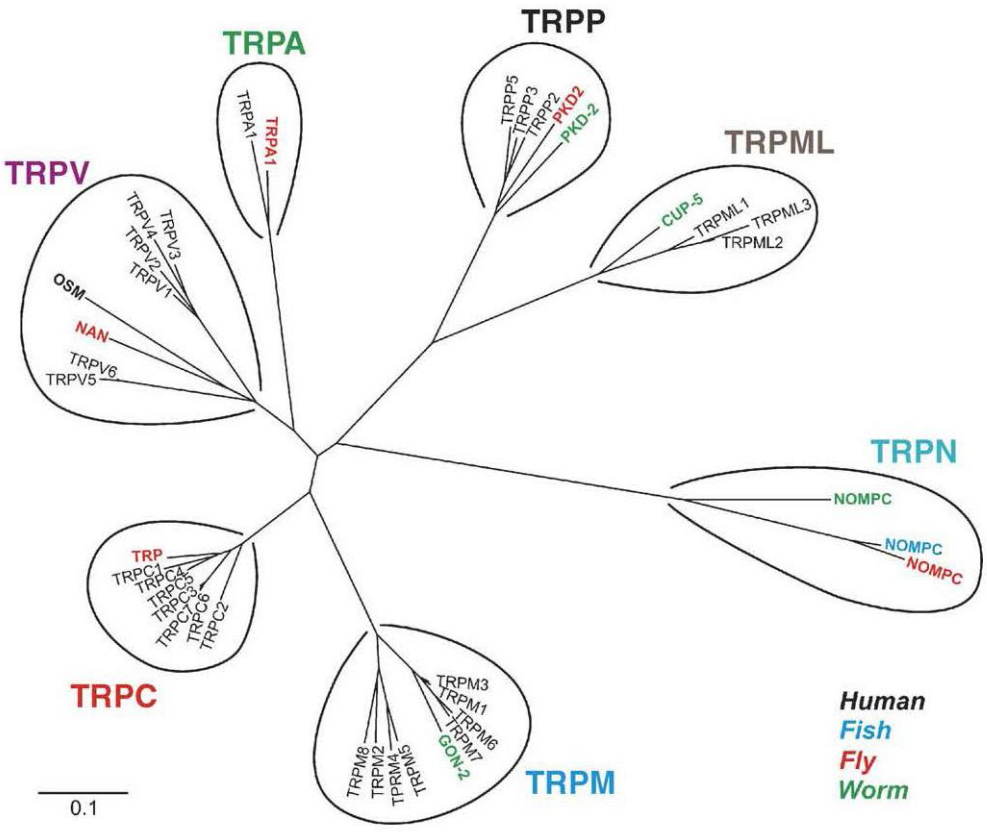

Figure 1.3: **Phylogenetic tree of the TRP superfamily.** *Reprinted from Cell Calcium, Vol. 38, Pedersen SF, et al., TRP channels: An overview, 233-252, Copyright (2005), with permission from Elsevier.* (Ref. 17)

All members of TRPs have an intracellular N- and C-terminus, as well as six transmembrane domains (TDs), of which TD 5 and 6 are necessary for the ion channels' pore formation. They show high functional variations in their selectivity for cation permeability (Figure 1.4)[17; 18]. All TRPCs and some other TRP proteins contain a 25-amino-acid domain with a C-terminus invariant sequence EWKFAR, the so-called TRP

box. Together, TRPC, TRPV, and TRPA display characteristic ankyrin repeats contained in the N-terminus[13]. Differences of sequence can be found in the N- and C-terminus as well as in the loops connecting the transmembrane domains. In the region of the channel pore, the sequence of amino acids is the most conserved[19].

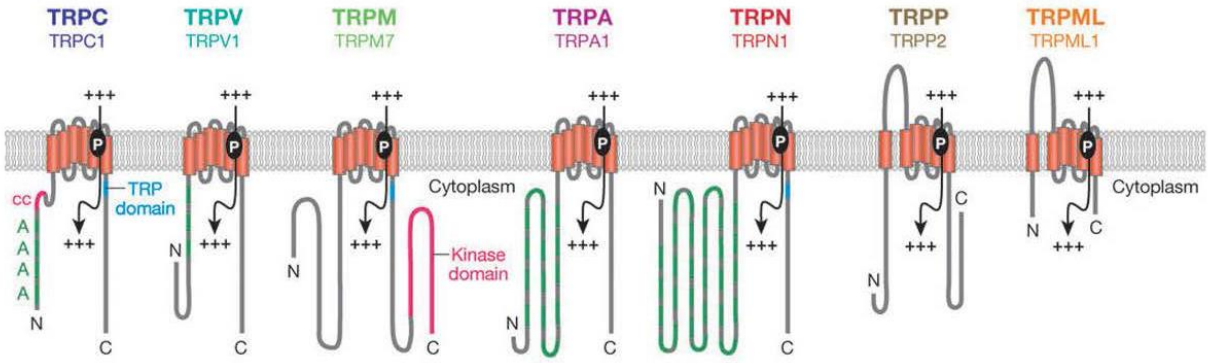

***Figure 1.4:* Structures of the different TRPs.** A, ankyrin repeats; cc, coiled-coil domain; P, pore loop. *Adapted with permission of Annual Reviews, Inc., from Annual Review of Biochemistry, Vol. 76, Venkatachalam K, et al., TRP Channels, Copyright (2007); permission conveyed through Copyright Clearance Center, Inc.* (Ref.18)

The TRPC subfamily is one of the main members of the TRP families. Although TRPC channels were the first TRP channels to be cloned and characterized in mammals, their physiological role is still not fully clear. All members of the TRPC family have similar structures. There are four ankyrin domains at the N-terminus followed by a so-called "coiled-coil" region (Figures 1.4 and 1.5). The subsequent transmembrane region is followed by a highly conserved TRP domain at the C-terminus. This region is followed by calmodulin and the IP3 receptor binding region (CIRB), which binds to phosphoinositide (Figure 1.5). Of all the TRP channels, the TRPC channels are most similar to the Drosophila TRP channels and are therefore referred to as "classical" or "canonical" as indicated by the letter "C" in their name [20; 21]. TRPCs are Ca^{2+}-permeable nonselective cation channels and include seven subtypes (TRPC1-7). Based on the similarity of the amino acid sequences and known physiological effects, the TRPC family can be divided into four subgroups: TRPC3/6/7, TRPC4/5, TRPC1 and TRPC2. TRPC1 is sometimes included in the TRPC4/5 subgroup, and TRPC2 is not expressed in humans[22; 23; 24]. While most TRPC subunits can form functional homomeric channels, heteromerization of TRPC channel subunits of either the same subfamily or different subfamilies has been widely observed to extend functional diversity [25; 26; 27; 28; 29; 30].

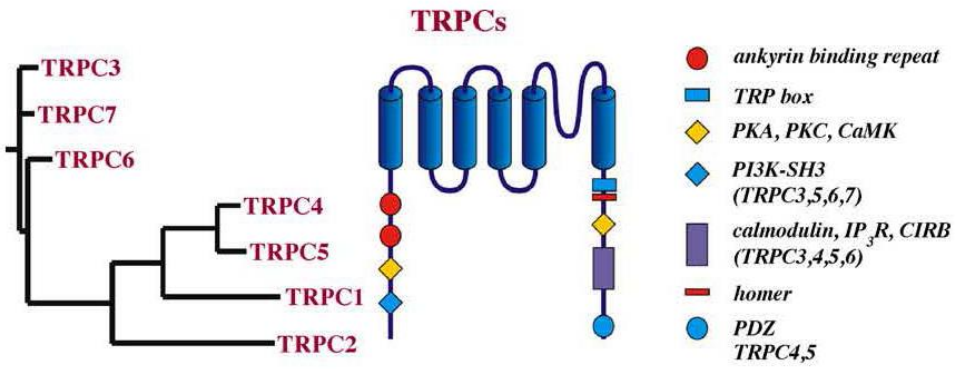

Figure 1.5: **Structure of TRPC family members.** *Reprinted from Cell Calcium, Vol. 38, Pedersen SF, et al., TRP channels: An overview, 233-252, Copyright (2005), with permission from Elsevier.* (Ref. 17)

1.3 TRPC and kidney

Interestingly, TRPC genes have been implicated in renal fibrosis. TRPC6 is widely expressed in renal tissues, including glomerular podocytes, mesangial cells, endothelial cells, tubulointerstitial vascular and epithelial cells, as well as in renal blood vessels [31]. TRPC6 is one of the podocyte slit-diaphragm proteins associated with proteinuria, which is mainly mediated by Ca^{2+} influx [32]. TRPC6, nephrin, podocin and CD2AP directly or indirectly interact with α-actinin-4 to maintain the integrity of the glomerular filtration barrier [32; 33]. Podocyte TRPC6 channels play a role in inherited focal segmental glomerulosclerosis [21]. Moreover, angiotension II (Ang II), known as an important causal driver of chronic kidney disease, can rapidly activate and upregulate the expression of TRPC6 in podocytes. Finally, up-regulation of TRPC3 and TRPC6 expression has been reported in UUO kidneys [34]. As a result, the intracellular Ca^{2+} concentration increases and eventually leads to podocyte apoptosis and progressive kidney failure [35; 36].

TRPC3 has been shown to be involved in rat kidney fibroblast proliferation and myofibroblast differentiation *in vitro* [37]. Furthermore, *in vivo* ablation of *Trpc3* in mice or pharmacologic inhibition of TRPC3 by the pyrazole compound Pyr3 diminished renal fibrosis in the UUO model [37]. To address the potential interplay between TRPC3 and TRPC6 in the fibrotic process, *Trpc3* and *Trpc6* single-knockout mice were compared with *Trpc3/6* double-knockout mice [34]. Interestingly, knockout of both *Trpc3* and *Trpc6* did not diminish UUO-induced fibrosis more than deletion of *Trpc6* alone [34]. BTP2, an inhibitor of several TRPC channels, including TRPC3 and TRPC6, had an effect similar

to that of a *Trpc6* knockout on fibrosis. In addition, BTP2 attenuated the up-regulation of *Trpc6* expression, which suggests that TRPC6 channel activity may induce its own gene expression in the UUO model and play an important role in promoting fibrosis [5]. In line with this, genomic deletion of TRPC6 has been observed to inhibit renal fibrosis after UUO in mice [34] and rats [38]. The anti-fibrotic effects were explained by a role for TRPC3/6 in hetero-tetramers (with or without the contribution of other TRPC channels) in interstitial fibroblast activation, differentiation, and proliferation [5]. Alternatively, they may be explained by increased homomeric TRPC6 channel activity due to their own increased gene expression in the UUO model. However, it is also possible that up- or downregulation of other TRPCs, e.g. in myofibroblast or other cell types, could play critical roles. For example, diabetic kidneys show reduced TRPC1 expression [39], which together with increased TRPC6 activity in podocytes could contribute to glomerulopathy [40; 41; 42]. *Trcp6*-deficiency has also been found to exert some renoprotective benefits such as the blunting of an increase in basal calcium in podocytes, reduced foot process damage, and a reduction in nephrin shedding in the streptozotocin (STZ)-induced diabetic Dahl salt-sensitive (Dahl SS) rat model, a type 1 diabetes mellitus model of diabetic nephropathy [43]. Given that the TRPCs have the ability to form homo- and heteromers, it is very likely that other TRPC family members additionally contribute to the formation of nephropathy in mouse and man. For example, pharmacological inhibition of TRPC5 has been found to delay progression of kidney disease due to hypertension [44].

The metabolic syndrome characterized by hypertension, hypoglycemia and lipedema is a complex disease leading to kidney disease. The New Zealand Obese (NZO) mouse represents one of the most thoroughly investigated polygenic models for the human metabolic syndrome and type 2 diabetes. It presents the main characteristics of the disease complex, including early-onset obesity, insulin resistance, dyslipidemia, and hypertension [45; 46; 47]. To the best of my knowledge, no studies have been reported on renal expression of TRPC channels in this model and their putative role in CKD progression.

1.4 Unilateral ureteral obstruction model

The unilateral ureteral obstruction (UUO) model is a standard and widely used experimental model of renal interstitial fibrosis (for review see [48]). Ureteral obstruction results in marked renal hemodynamic and metabolic changes, followed by tubular injury and cell death by apoptosis or necrosis in conjunction with an infiltration of macrophages and other inflammatory cells into the renal interstitium. Proliferation of fibroblasts and transformed myofibroblasts are responsible for the excessive production of extracellular matrix and accelerated renal fibrosis. Phenotypic transition of resident renal tubular cells, endothelial cells, and pericytes has also been implicated in this process [48]. The use of genetically engineered mice has greatly expanded the utility of the model for studying molecular mechanisms underlying the renal response to UUO.

1.5 Hypothesis and aims of the study

The aim of the study here was to understand the therapeutic potential of TRPC6 inhibition in renal fibrosis underlying the progression of CKD to end-stage renal disease. The hypothesis that up-regulation of renal TRPC6 is a common feature in UUO kidneys contributing to renal fibrosis and immune cell infiltration in mice was tested. The UUO model was used to induce renal fibrosis and immune cell infiltration, and the expression of TRPC channels in the kidneys of wild-type (WT) and *Trpc6*-knockout (*Trpc6*$^{-/-}$) mice was analyzed. Furthermore, the therapeutic efficiency of TRPC6 inhibition was evaluated in obstructive nephropathy using *Trpc6*$^{-/-}$ mice. The NZO mouse model[45; 46; 47; 49] was used to evaluate UUO nephropathy as well as the regulation of TRPC channel expression in an inbred obese mouse strain carrying susceptibility genes for diabetes and hypertension.

Chapter 2
Materials and Methods

2.1 Animals

Male *Trpc6*$^{-/-}$ mice (24.51 ± 2.73 g body weight (b.w.), n=31, 9-12 weeks old) and age-matched WT controls (25.69 ± 1.79 g b.w., n=32, p>0.05) were used (Figure 2.1A and B). The *Trpc6*$^{-/-}$ mice were generated on C57BL/6J:129/Sv genetic background and characterized previously [50]. Since 129Sv and C57BL/6J mice display similar renal damage in the UUO model [51], C57BL/6J mice were chosen as control *Trpc6*$^{+/+}$ (WT) mice. Age-matched male NZO mice (Figure 2.1C) which were obese (39.90 ± 4.11 g b.w., n=15, p<0.05 *versus* both WT and *Trpc6*$^{-/-}$ mice) and carried susceptibility genes (from the NZO/BomHIDife genetic background) for obesity, diabetes and hypertension were used [45; 46; 47; 49]. All mice were bred and raised in the Max-Rubner-Laboratory (MRL) of the German Institute of Human Nutrition (Nuthetal, Germany). The mice were housed in groups of three to five and single housing was applied 7 days before and after the UUO surgery to ensure uniformity. The mice were reared under specific-pathogen-free (SPF) conditions in individually ventilated cages (IVC) with a diurnal 12 h light and dark cycle (lights on at 06:00 h) at a temperature of 21±1°C. All animals had free access to water and food. The mice were housed and handled according to good animal practice as defined by the Federation of European Laboratory Animal Science Associations (FELASA)[52] and the national welfare body GV-SOLAS[53]. Animal care followed American Physiological Society guidelines [54], and all protocols were locally approved (LUGV Brandenburg, Germany; Permit-Number: 2347-7-2016).

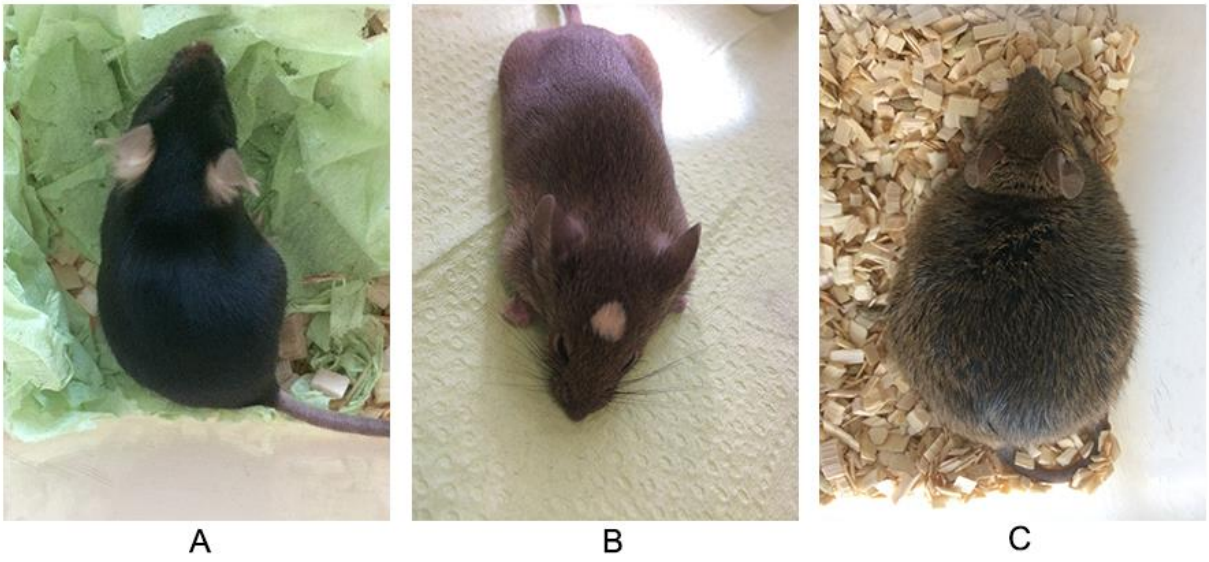

Figure 2.1: **Experimental mice.** (A) C57BL/6J mice. (B) *Trpc6*$^{-/-}$ mice. (C) NZO mice.

2.2 UUO model

All surgical procedures were performed under aseptic conditions. The mice were anesthetized with 2% isoflurane and placed on a heating pad to prevent hypothermia. After the depth of anesthesia was confirmed by a loss of reflexes (toe pinch), the anterior abdominal skin was shaved, wiped with 70% ethanol and 500 mg/kg metamizole (500 mg/ml, WDT) was injected intraperitoneally (i.p.). Eventually a midline laparotomy was conducted via an incision of the avascular linea alba and the left ureter was exposed. The ureter was then ligated twice close to the renal pelvis using a 5-0 polyglycolic acid (PGA) suture wire (Resorba®), and subsequently, 0.05 ml of a 10% enrofloxacine solution (Baytril, Bayer) was applied in the abdominal cavity. Sham operation was performed without ureteral ligation. The linea alba and skin were closed separately. The wound was sanitized with a silver aluminium spray (Henry Schein®), and 1 ml of warm (37°C) isotonic sodium chloride solution (Berlin-Chemie Menarini) was injected subcutaneously (s.c.). Subsequently, each mouse was placed in a cage in front of an infrared (IR) lamp and monitored until it recovered consciousness. For the following two days mice received metamizole (500mg/ml, Lichtenstein) in their drinking water with a final concentration of 1.33mg/ml. The tissue harvest occurred 7 days after the surgeries (UUO and sham). For this, mice were sacrificed with an overdose of isoflurane (1 ml/ml, CP-Pharma) and death was confirmed via a lack of reflex formation upon targeted provocation. The left kidneys

were excised and decapsulated for further analysis. The kidneys were transversely divided into two portions. Half of the kidney was immersed in a 4% phosphate-buffered paraformaldehyde (PFA) (Sigma) solution for histology, and the other half was snap-frozen in liquid nitrogen for RNA preparation.

2.3 Histology and immunohistochemistry

Paraffin-embedded kidneys were cut in three micrometer thick sections followed by deparaffination in sequential steps of xylene, ethanol solutions (100%, 96%, 70%) and a final rehydration step in water. For the morphological and histological analyses, Sirius red (SR) stains and Periodic acid Schiff (PAS) reactions were performed according to the manufacturer's protocols (Sigma). SR specifically stains collagen type 1 and 3 fibrils and allows a quantification of interstitial fibrosis. The PAS reaction allows visualization of the basement membranes of the capillary loops of the glomeruli, through which the glomerular damage can be evaluated.

For the immunohistochemical (IHC) analysis and the detection of the proteins of interest, the following procedure was conducted: antigen retrieval was achieved by immersing the samples in boiling sodium citrate buffer (MW-buffer, pH 6.0, S2031, DAKO) in a microwave. This included two 4 min steps and one 5 min step at room temperature in between. In order to block the endogenous peroxidase activity, the tissues were incubated in 3% H_2O_2 in purified water for 10 min. Furthermore, the tissue was perforated using Tris-buffered saline with tween 20 (TBST) buffer for 15 min and potential unspecific antibody binding was prevented via a 10 min blocking step with DAKO antibody diluent (S3022, DAKO). In between each of these steps, the samples were washed with a TBST buffer for 5 min and a final washing step with phosphate-buffered saline (PBS) before the incubation with the following primary antibodies: anti-F4/80 (rat monoclonal, 1:8000, MCA497GA, Serotec), anti-CD3 (rabbit polyclonal, 1:250, ab5690, Abcam), anti-alpha smooth muscle actin (αSMA) (rabbit polyclonal, 1:500, ab5694, Abcam), anti-vimentin (rabbit monoclonal, 1:2000, ab92547, Abcam), collagen type 4, alpha 1 (Col4α1) (rabbit polyclonal, 1:2000, ab6586, Abcam), anti-proliferating cell nuclear antigen (PCNA) (rabbit polyclonal, 1:1000, ab18197, Abcam) and anti-cleaved-caspase 3 (cCasp3) (rabbit polyclonal, 1:280, 9661S, Cell Signaling). All primary antibodies were diluted in DAKO

antibody diluent and incubated over night at 4°C except for the anti-CD3 antibody, whose incubation occurred at room temperature for 1 hour (h). After antibody incubation, the samples were washed three times with PBS (5 min each) and Histofine® Simple Stain™ MAX PO, which uses the 3,3'-diaminobenzidine (DAB) chromogen, was applied according to the manufacturer's protocol (Nichirei). This allowed the visualization of the proteins of relevance. Eventually, the tissue samples were counterstained with haematoxylin (Roth) and dehydrated in a sequence of ethanol solutions followed by a final xylene dehydration step. The slides were then sealed with mounting medium (Histokitt, 1025/500, Hecht) and stored until they were imaged.

2.4 Histological analyses

The kidneys of all the animals in each group were analyzed in a blinded manner to minimize the observer bias. All slides were scanned by a digital slide scanner (Pannoramic™ MIDI II, 3DHISTECH) (Figure 2.2). Images were taken with the software CaseViewer (3DHISTECH) at either 20x (all IHC stains) or 40x (PAS and SR). The cortex of each kidney sample was screened thoroughly starting at one end of the tissue and ending at the other. In order to achieve a concise quantification of the area of interest in a semiautomatic manner, an NIH ImageJ plug-in, previously generated by Gabriel Landini (university of Birmingham), was used. This plug-in allows a color threshold to be set and the generation of macros that can be applied individually to all stored images of each stain to guarantee consistency. The mesangial expansion and thus glomerular damage could be visualized with the PAS stain. For this, the PAS^+ area of at least 20 glomeruli in each animal was analyzed. This was done by assessing the glomerular perimeter and normalizing the positively stained area to the glomerular capillary tuft area. The SR stain allowed the quantification of fibrosis in the renal cortex. At least 15 pictures of each SR-stained kidney were taken and the total positively stained area of each visual field was quantified. The F4/80, vimentin, αSMA, Col4α1 positive areas were measured in the same manner whereas $CD3^+$ as well as $PCNA^+$ cells were counted individually using the ImageJ threshold plug-in as previously mentioned.

Figure 2.2: **Pannoramic™ Digital Slide Scanner** (Pannoramic™ MIDI II)**.** The scanner scans automatically up to 12 slides in one run and supports the Carl Zeiss objectives.

2.5 Quantitative real-time (qRT)-PCR

qRT-PCR was performed as described earlier [55]. Briefly, total RNA was isolated from the snap-frozen kidney cortex after homogenization with a Precellys 24 homogenizer (Peqlab) using the RNeasy RNA isolation kit (Qiagen). RNA quality and concentration were determined by a NanoDrop-1000 spectrophotometer (Thermo Fisher Scientific). Two micrograms of total renal RNA were transcribed to cDNA (Applied Biosystems). Quantitative analysis of target mRNA expression was calculated using the relative standard curve method. TaqMan and SYBR green analysis was conducted using an Applied Biosystems 7500 Sequence Detector (Applied Biosystems). The expression levels were normalized to GAPDH (glyceraldehyde-3-phosphate dehydrogenase) and eEF1α1 (eukaryotic translation elongation factor 1 alpha 1), and mean Ct values of each groups are reported (Figure 2.3). Primer sequences are provided in Table 2.1.

Table 2.1: **Details of specific primers used in real-time PCR experiments.**

Gene	Forward	Reverse
GAPDH	5'-TGT GTC CGT CGT GGA TCT GA-3'	5'-CCT GCT TCA CCA CCT TCT TGA-3'
	Probe: 5'-6-FAM-TGC CGC CTG GAG AAA CCT GCC-TAMRA -3'	

eEF1α1	5’-TCG TCG TAA TCG GAC ACG TA-3’	5’-CAG CAG CCT CCT TCT CAA AC-3’
Trpc1	5’-TGG GCC CAC TGC AGA TTT CAA-3’	5’-AAG ATG GCC ACG TGC GCT AAG GAG-3’
Trpc2	5’-TTG CCT CCC TCA TCT TCC TCA CCA-3’	5’-CCG CAA GCC CTC GAT CCA CAC CT-3’
Trpc3	5’-AGC CGA GCC CCT GGA AAG ACA C-3’	5’-CCG ATG GCG AGG AAT GGA AGA C-3’
Trpc4	5’-GGG CGG CGT GCT GCT GAT-3’	5’-CCG CGT TGG CTG ACT GTA TTG TAG-3’
Trpc5	5’-AAC TCC CTC TAC CTG GCA ACT A-3’	5’-GGA TAT GAG ACG CAA CGA ACT T-3’
Trpc6	5’-GAC CGT TCA TGA AGT TTG TAG CAC-3’	5’-AGT ATT CTT TGG GGC CTT GAG TCC-3’
Trpc7(primer1)	5’-GTG GGC GTG CTG GAC CTG-3’	5’-AGA CTG TTG CCG TAA GCC TGA GAG-3’
Trpc7(primer2)	5’-GCG GCC CCA TGA CTA CTT C-3’	5’-TGG ATA GGG ACA GGT AGG CG-3’
Trpc7(primer3)	5’-CGT CCA AGT CTG AGC CGA AT-3’	5’-GGT TTG TCC TAG CTT GCT GC-3’
Col1α1	5’-CAT GTT CAG CTT TGT GGA CCT-3’	5’-GCA GCT GAC TTC AGG GAT GT-3’
Col3α1	5’-CTC ACC CTT CTT CAT CCC ACT CTT A-3’	5’-ACA TGG TTC TGG CTT CCA GAC AT-3’
Col4α1	5’-TTA AAG G ACT CCA GGG ACC AC-3’	5’-CCC ACT GAG CCT GTC ACA C-3’
αSMA (ACTA2)	5’-ACT GGG ACG ACA TGG AAA AG-3’	5’-CAT CTC CAG AGT CCA GCA CA-3’
TGFβ1	5’-TGG AGC AAC ATG TGG AAC TC-3’	5’-GTC AGC AGC CGG TTA CCA-3’
VCAM1	5’-CTG GGA AGC TGG AAC GAA GT-3’	5’-GCC AAA CAC TTG ACC GTG AC-3’
ICAM1	5’-CTG GGC TTG GAG ACT CAG TG-3’	5’-CCA CAC TCT CCG GAA ACG AA-3’
MCP1 (CCL2)	5’-TTA AAA ACC TGG ATC GGA ACC AA-3’	5’-GCA TTA GCT TCA GAT TTA CGG GT-3’
IL1β	5’-GAA ATG CCA CCT TTT GAC AGT G-3’	5’-TGG ATG CTC TCA TCA GGA CAG-3’

IL6	5'-ATC CTC TGG AAC CCC ACA C-3'	5'-GAA CTT TCG TAC TGA TCC TCG TG-3'
TNFα	5'-CTG AAC TTC GGG GTG ATC GG-3'	5'-GGC TTG TCA CTC GAA TTT TGA GA-3'

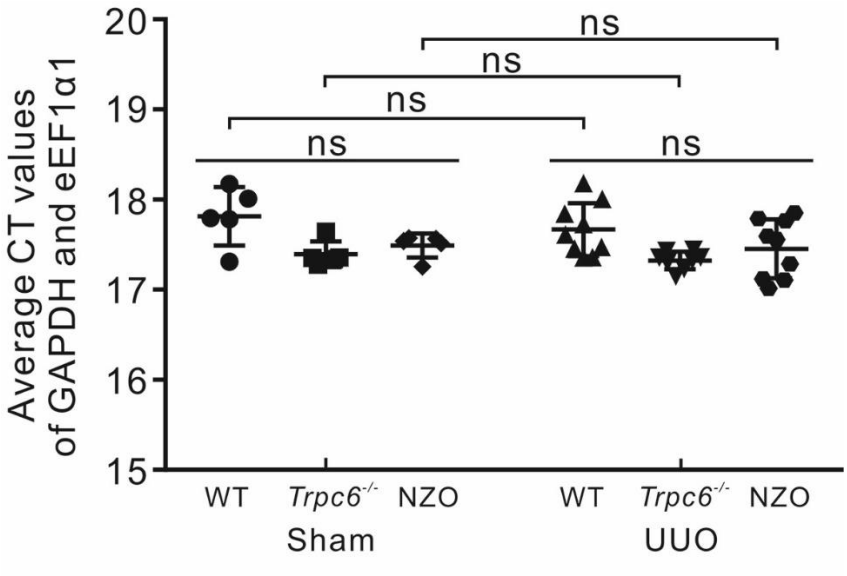

Figure 2.3: **Average CT values of two housekeeping genes:** Glyceraldehyde-3-Phosphate Dehydrogenase (GAPDH) and Eukaryotic Translation Elongation Factor 1 alpha 1 (eEF1α1). There is no statistical significance between sham-operated groups and UUO-operated groups in wild-type (WT), *Trpc6*$^{-/-}$ and NZO mice. ns, *not significant.*

2.6 Statistical analyses

Statistical analyses were performed using GraphPad Prism 7.0 (GraphPad Software). All data are presented as mean ± SD and *p*-values of <0.05 were considered as statistically significant. The *p*-values in the figures are denoted as follows: ns *p>0.05*, **p*<0.05, ***p*<0.01, ****p*<0.001 and *****p*<0.0001. Data were analyzed by regular two-way ANOVA with Bonferroni's multiple comparisons test. Data with two groups were tested by two-sided unpaired t-test (data with normal distribution).

Chapter 3
Results

3.1 UUO induces renal damage and apoptosis

Urinary tract obstruction led to hydronephrosis, caused by urine stasis in the renal pelvis or calyces, in all UUO kidneys (Figure 3.1). The glomerular and tubular basement membrane as well as the brush border of the proximal tubules were visualized by periodic acid Schiff (PAS) staining. The increases in mesangial matrix deposition in the glomeruli in both WT UUO and *Trpc6*$^{-/-}$ UUO *versus* sham kidneys implicates renal damage induced by UUO (Figure 3.2A and B). Moreover, there were no differences in glomerular injury in WT *versus* *Trpc6*$^{-/-}$ kidneys upon UUO, indicating similar glomerular damage in both genotypes (Figure 3.2A and B).

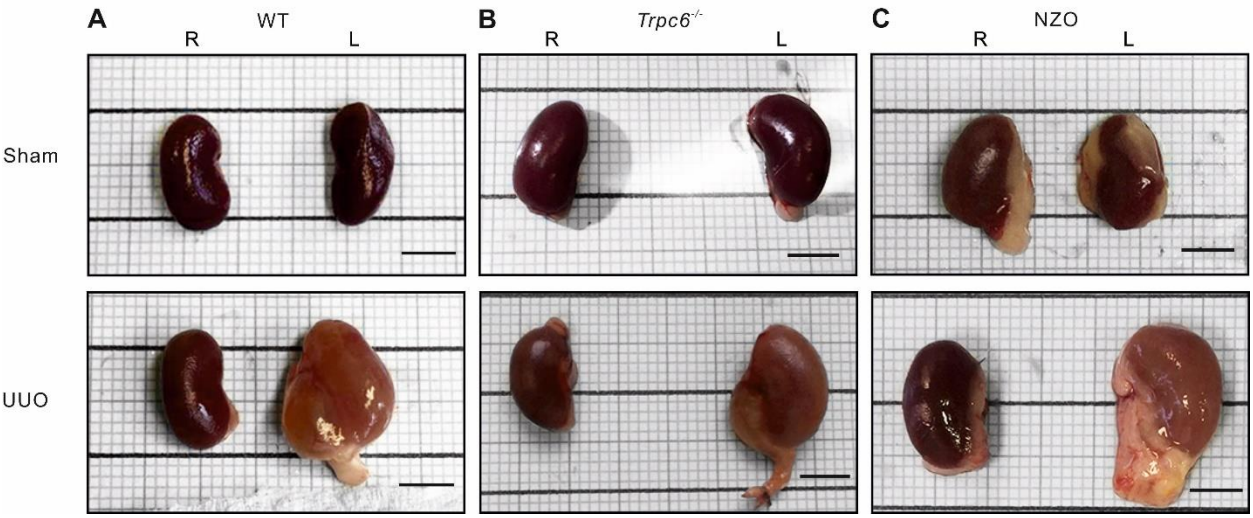

Figure 3.1: **Macroscopic analysis of the kidneys.** Images of the left (L) and right (R) kidneys of **(A)** Wild type (WT) mice, **(B)** Trpc6$^{-/-}$ mice and **(C)** NZO mice. The left UUO kidneys of all mice increased in size (hydronephrosis) compared to the sham kidneys. Scale bar: 1cm.

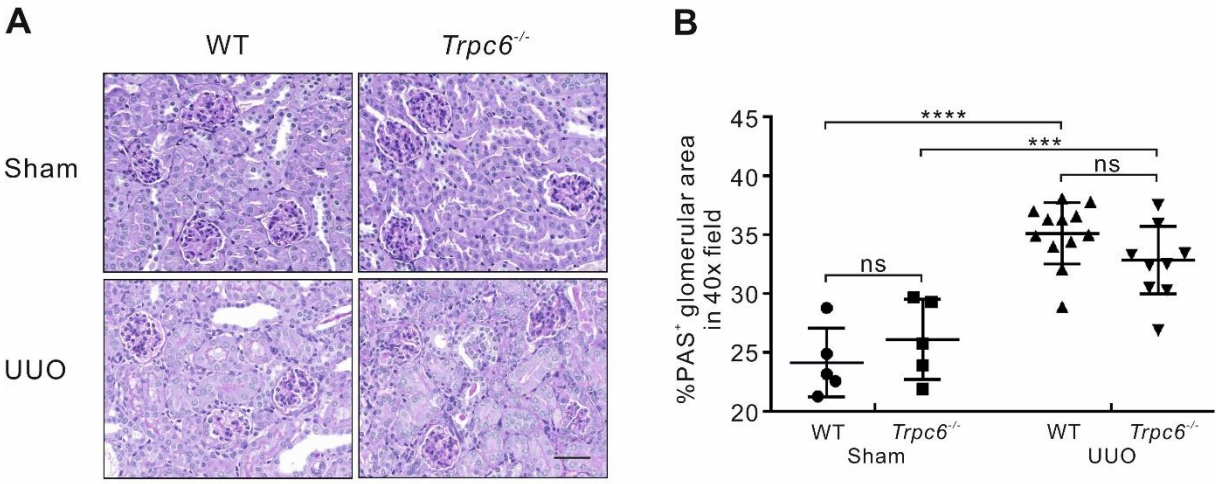

Figure 3.2: **PAS stained kidneys. (A):** Kidneys stained with the periodic acid Schiff (PAS) stain to detect glomerular damage. **(B)** Quantification of the PAS positive areas in the kidneys. All images were taken at a magnification of 40x. Scale bar: 50 µm. All values are *means* ± *SD*. ns $p>0.05$, ***$p<0.001$ and ****$p<0.0001$. *Wild type* (WT) and *Trpc6*$^{-/-}$ sham groups included n=5 kidney samples each. *WT* and *Trpc6*$^{-/-}$ UUO-treated groups encompassed n=12 (*WT*) and n=11 (*Trpc6*$^{-/-}$) kidney samples. ns, *not significant*.

Next, sections of the kidneys were stained with antibodies against proliferating cell nuclear antigen (PCNA, to determine the mean proliferation index of PCNA) (Figure 3.3A) and programmed cell death marker cleaved-caspase 3 (cCasp3) (Figure 3.3C). UUO-induced increases in PCNA positive (PCNA^{+}) cells and cCasp3 positive (cCasp3^{+}) cells were clearly visible in the kidneys of both WT and *Trpc6*$^{-/-}$ mice. Although there was no difference in the number of PCNA^{+} cells between UUO WT and *Trpc6*$^{-/-}$ kidneys (Figure 3.3B), fewer cCasp3 positive cells were found in *Trpc6*$^{-/-}$ UUO kidneys compared to WT UUO kidneys, indicating that ureteral obstructed *Trpc6*$^{-/-}$ kidneys show less apoptosis compared to obstructed WT kidneys (Figure 3.3D).

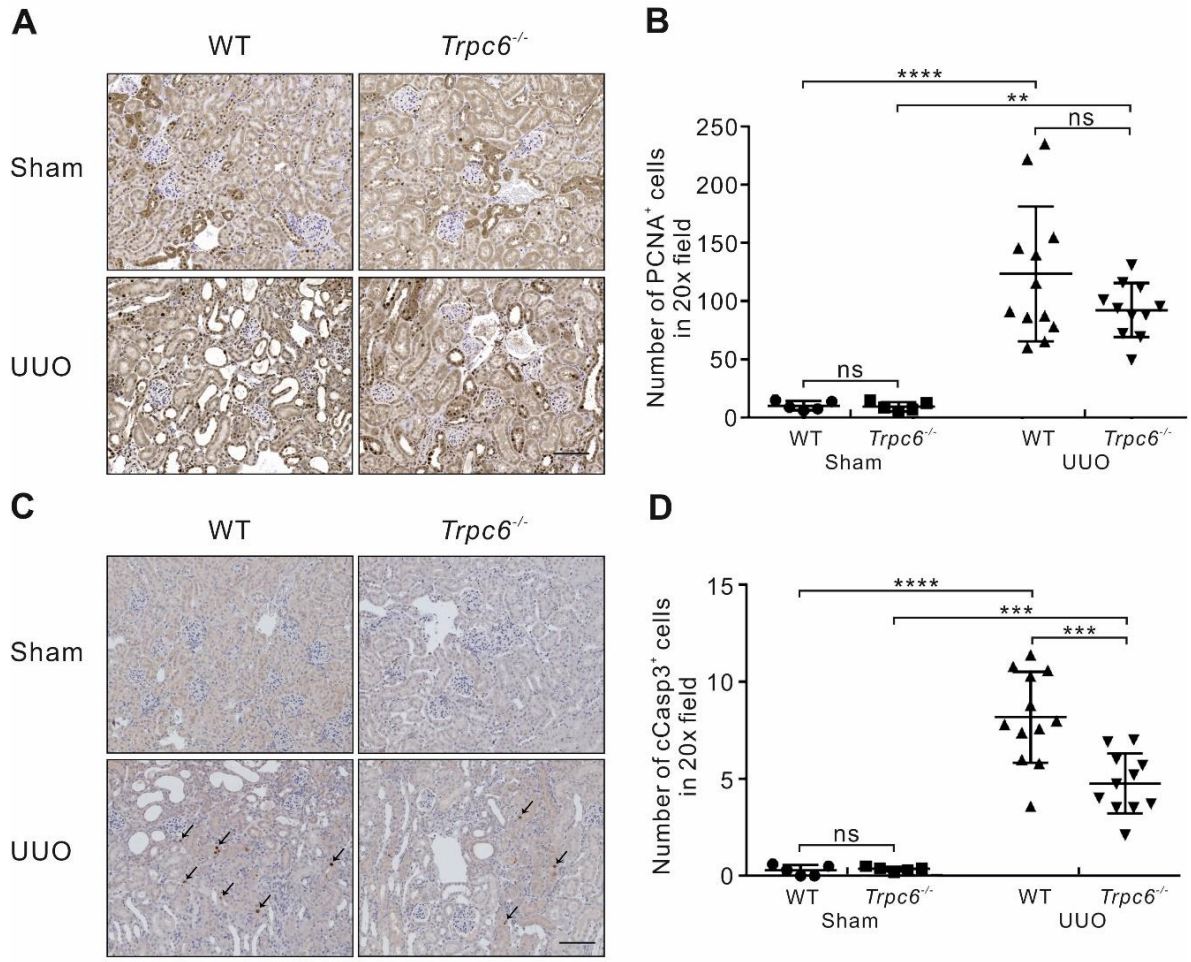

Figure 3.3: **Markers of proliferation and apoptosis. (A)** Proliferating cell nuclear antigen (PCNA) antibody staining: marker of cell regeneration. **(B)** Quantification of renal cells positively stained for PCNA. **(C)** Cleaved-caspase 3 (cCasp3) antibody staining: marker of apoptosis. (Arrows: cCasp3$^+$ cells) **(D)** Quantification of renal cells positively stained for cCasp3. All images were taken at a magnification of 20x. Scale bar: 100 µm. All values are *means* ± *SD*. ns *p>0.05*, ***p<0.001 and ****p<0.0001. *Wild type* (WT) and *Trpc6*$^{-/-}$ sham groups included n=5 kidney samples each. *WT* and *Trpc6*$^{-/-}$ UUO-treated groups encompassed n=12 (*WT*) and n=11 (*Trpc6*$^{-/-}$) kidney samples. ns, *not significant.*

3.2 Role of TRPC6-deficiency in renal inflammation

UUO induces immune responses such as infiltration of blood cells leading to renal inflammation [48]). Therefore, it was determined whether *Trpc6*-deletion can affect renal immune infiltration as well as mRNA expression of pro-inflammatory markers in the kidneys. Antibodies against the macrophage marker F4/80 and the T-cell marker CD3 were applied in IHC analyses. UUO caused immune cell infiltration in WT and *Trpc6*$^{-/-}$ kidneys, as assessed by F4/80 positive (F4/80$^+$) areas and the numbers of CD3 positive (CD3$^+$) cells in the respective kidney sections (Figure 3.4A-D). However, this infiltration

was smaller in *Trcp6*$^{-/-}$ UUO kidneys compared to WT UUO kidneys (Figure 3.4A-D), which indicates a protective effect when TRPC6 is absent.

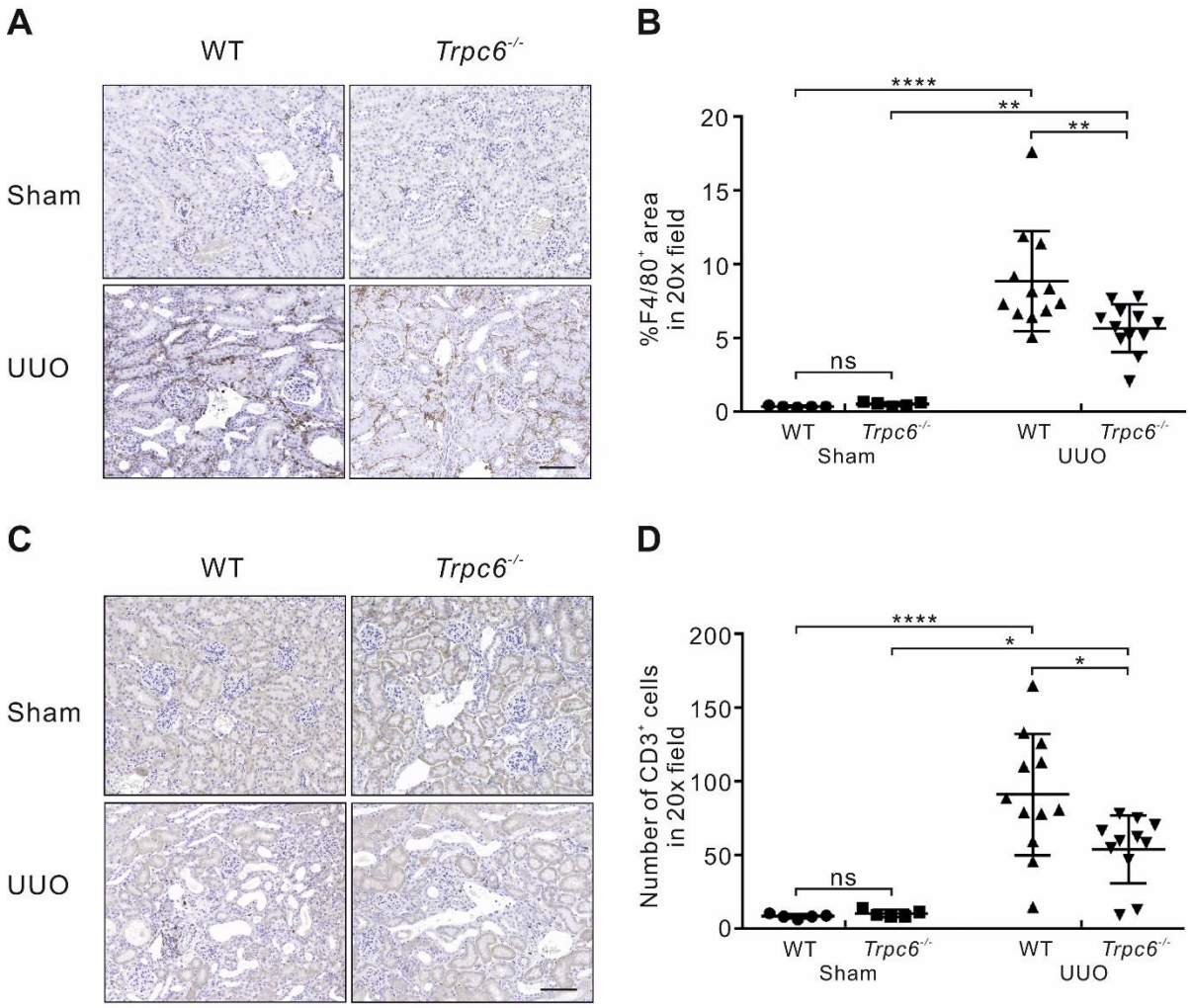

Figure 3.4: **Markers of inflammation in wild-type (WT) and *Trpc6*$^{-/-}$ kidneys. (A)** F4/80 antibody staining: macrophage marker. **(B)** Quantification of the F4/80 positive areas. **(C)** CD3 antibody staining: T-cell marker. **(D)** Quantification of the CD3 positive cells. WT and *Trpc6*$^{-/-}$ l UUO-treated groups encompassed n=12 (WT) and n=11 (*Trpc6*$^{-/-}$) kidney samples. All quantification data are *means* ± *SD*. ns $p>0.05$, *$p<0.05$, **$p<0.01$ ***$p<0.001$ and ****$p<0.0001$. WT and *Trpc6*$^{-/-}$ sham groups included n=5 kidney samples each. All images were taken at a magnification of 20x. Scale bar: 100 µm. ns, *not significant*.

Next, qRT-PCR was applied to analyse mRNA expression of the pro-inflammatory markers interleukin 1 beta (IL1β), interleukin 6 (IL6), tumor necrosis factor alpha (TNFα), intercellular adhesion molecule 1 (ICAM1), vascular cell adhesion molecule 1 (VCAM1), and monocyte chemotactic protein 1 (MCP1). As a result, all mentioned markers were found to be significantly increased upon UUO in the renal cortex of both WT and *Trpc6*$^{-/-}$

kidneys (Figure 3.5). There were no differences observed between mRNA expression of IL1β, IL6 and TNFα in *Trpc6*$^{-/-}$ UUO and WT UUO kidneys (Figure 3.5A-C). However, it was found that *Trpc6*$^{-/-}$ UUO kidneys displayed increased mRNA expression levels of ICAM1, VCAM1 and MCP1 relative to WT UUO kidneys (Figure 3.5D-F).

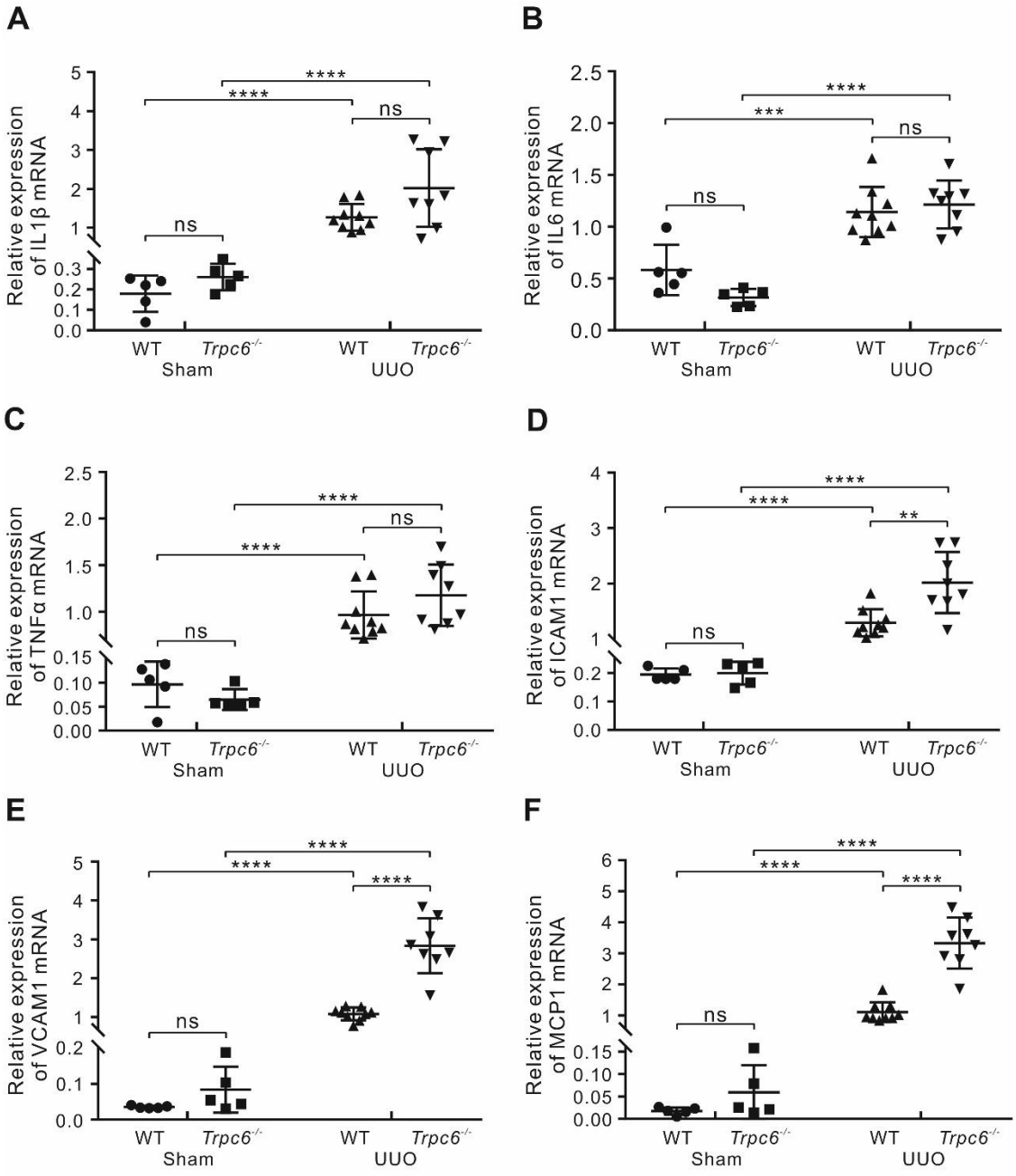

***Figure 3.5*: Expression of inflammatory markers in wild-type (WT) and *Trpc6*$^{-/-}$ kidneys.** Renal mRNA levels of **(A)** interleukin 1 beta (IL1β), **(B)** interleukin 6 (IL6), **(C)** tumor necrosis factor alpha (TNFα), **(D)** intercellular adhesion molecule 1 (ICAM1), **(E)** vascular cell adhesion molecule 1 (VCAM1) and **(F)** monocyte chemotactic protein 1 (MCP1) in sham-operated groups and in UUO-operated groups. Renal mRNA expression data were determined in n=5 each for sham-operated WT and *Trpc6*$^{-/-}$ kidneys, n=9 for UUO-operated WT kidneys and n=8 for UUO-operated *Trpc6*$^{-/-}$ kidneys. The relative standard curve method was used for relative quantification. All data are *means* ± *SD*, ns *p>0.05*, **p<0.05*, ***p*<0.01, ****p*<0.001, *****p*<0.0001. ns, *not significant*.

3.3 Role of TRPC6-deficiency in renal fibrosis

To examine a possible role of TRPC6-deficiency in renal fibrosis, histological analysis including IHC and gene expression measured by qRT-PCR were performed. A *Sirius red* (SR) stain was performed and SR positive (SR^+) areas were quantified (Figure 3.6A, B) to assess the degree of collagen deposition in the kidneys. Sham-treated kidneys of either genotype exhibited only small areas of SR^+ areas (Figure 3.6A). In contrast, WT UUO kidneys displayed a 6fold increase in SR^+ areas compared to controls. This increase in collagen deposition was smaller in *Trpc6*$^{-/-}$ UUO kidneys compared to WT UUO kidneys (Figure 3.6B). Next, IHC studies were performed using antibodies against collagen type 4 alpha 1 (Col4α1) to determine the level of fibrosis, the mesenchymal marker vimentin to identify epithelial-to-mesenchymal transition (EMT) of tubular epithelial cells, and alpha smooth muscle actin (αSMA) to detect myofibroblasts and mesangial cells as indicators of cell types involved in fibrosis (Figure 3.6C-H). As a result, a significant increase was observed in the Col4α1 positive ($Col4α1^+$) area in UUO kidneys compared to sham kidneys of both genotypes (Figure 3.6C, D). However, this increase in the Col4α1 positive ($Col4α1^+$) area was smaller in *Trpc6*$^{-/-}$ UUO kidneys compared to WT UUO kidneys (Figure 3.6C, D). Furthermore, a marked increase in the vimentin positive ($vimentin^+$) area (Figure 3.6E, F) and the αSMA positive ($αSMA^+$) area (Figure 3.6G, H) was observed in UUO kidneys of both genotypes. Again, the increase in $vimentin^+$ mesenchymal cells and $αSMA^+$ myofibroblasts was smaller in *Trpc6*$^{-/-}$ UUO kidneys compared to WT UUO kidneys (Figure 3.6E-H). Taken together, these data suggest a protective effect in renal fibrosis when TRPC6 is absent.

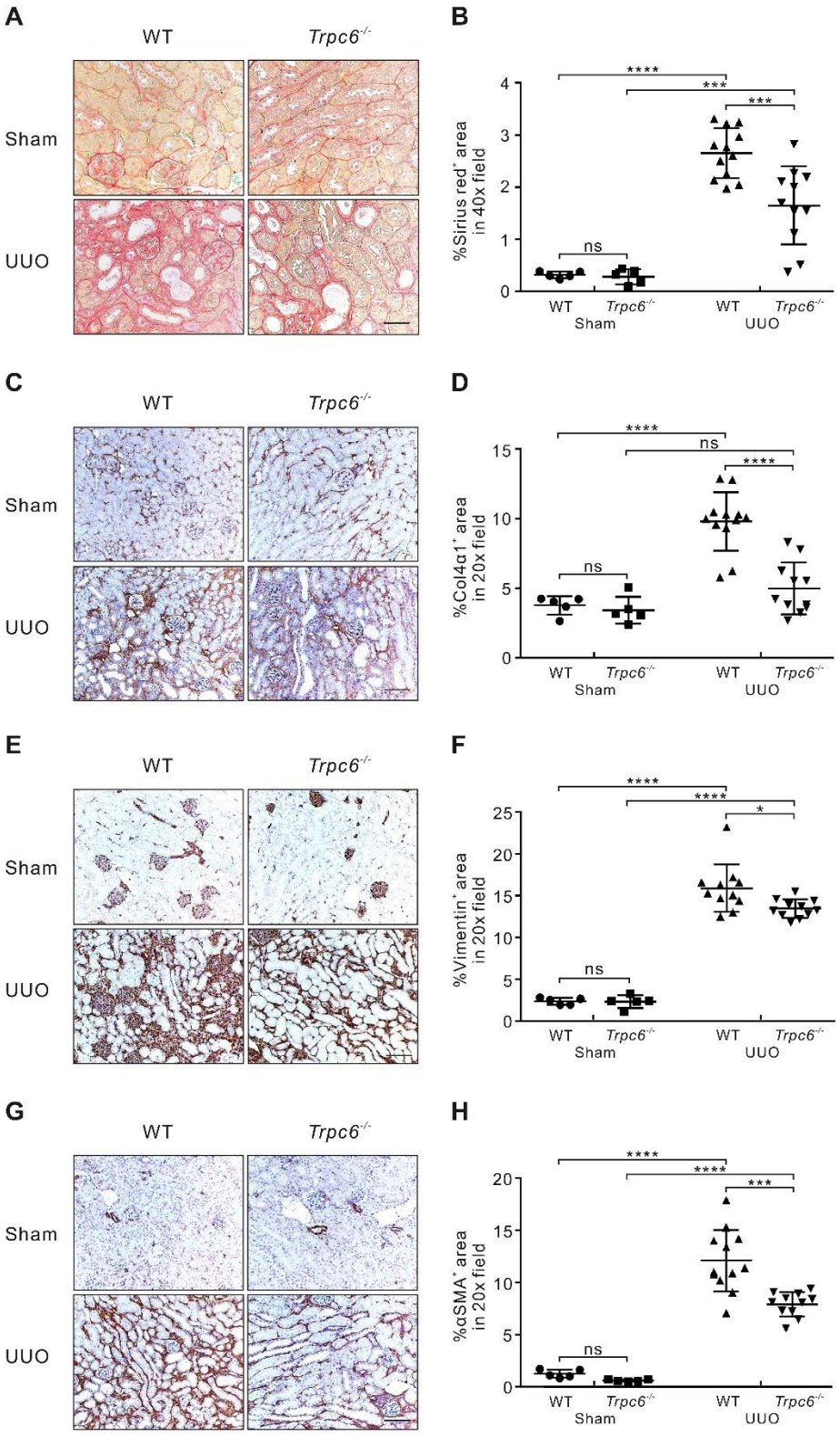

***Figure 3.6*: Expression of fibrosis markers. (A)** Sirius red (SR) staining (40x, Scale bar: 50 µm). **(B)** Quantification of the SR positive areas. **(C)** Collagen type 4, alpha 1 (Col4α1) antibody staining: fibrosis marker (20x, Scale bar: 100 µm). **(D)** Quantification of the Col4α1 positive areas. **(E)** Vimentin antibody staining: mesenchymal marker (20x, Scale bar: 100 µm). **(F)** Quantification of the vimentin positive areas. **(G)** Alpha smooth muscle actin (αSMA) antibody staining: myofibroblast marker (20x, Scale bar: 100 µm). **(H)** Quantification of the αSMA positive areas. Wild type (WT) and *Trpc6*$^{-/-}$ sham groups included n=5 kidney samples each. WT and *Trpc6*$^{-/-}$ UUO-treated groups encompassed n=12 (WT) and n=11 (*Trpc6*$^{-/-}$) kidney samples. All quantification data are *means* ± *SD*. ns $p>0.05$, *$p<0.05$, ***$p<0.001$ and ****$p<0.0001$. ns, *not significant*.

Using qRT-PCR, the mRNA expression of pro-fibrotic markers in the renal cortex was analysed, including collagen type 1 alpha 1 (Col1α1), collagen type 3 alpha 1 (Col3α1), collagen type 4 alpha 1 (Col4α1), transforming growth factor beta 1 (TGFβ1) and αSMA (Figure 3.7). Whereas UUO caused increased mRNA expression of all pro-fibrotic

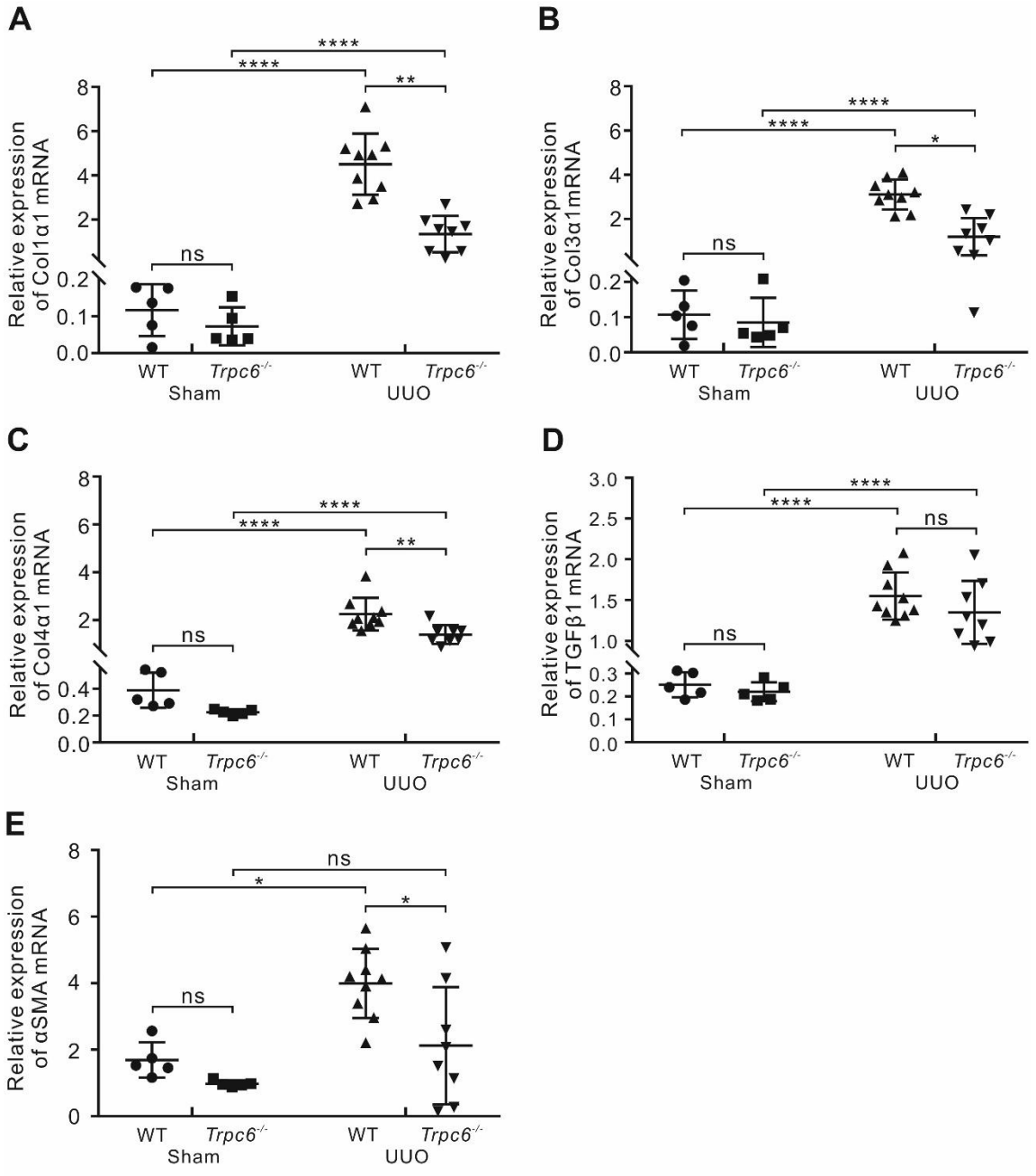

***Figure 3.7*: Expression of genes involved in renal fibrosis in kidneys of wild-type (WT) and *Trpc6*$^{-/-}$ mice.** Renal mRNA levels of **(A)** collagen type 1, alpha1 (Col1α1), **(B)** collagen type 3, alpha1 (Col3α1), **(C)** collagen type 4, alpha1 (Col4α1), **(D)** transforming growth factor beta 1 (TGFβ1) and **(E)** alpha smooth muscle actin (αSMA) in sham-operated groups and in UUO-operated groups. Renal mRNA expression data were determined in n=5 each for sham-operated WT and *Trpc6*$^{-/-}$ mice, n=9 for UUO-operated WT mice and n=8 for UUO-operated *Trpc6*$^{-/-}$ mice. The relative standard curve method was used for relative quantification. All data are *means* ± *SD*., ns *p>0.05*, **p<0.05*, ***p*<0.01, ****p*<0.001, *****p*<0.0001. ns, *not significant*.

markers in the renal cortex of WT mice (Figure 3.7A-E), *Trpc6*-deficiency UUO kidneys displayed only a significant increase in Col3α1, Col4α1 and TGFβ1 but not αSMA mRNA levels (Figure 3.7B, C, D). Comparing the mRNA expression of the aforementioned markers within the UUO-treated groups, all pro-fibrotic markers except TGFβ1 were found to be reduced in *Trcp6*$^{-/-}$ UUO kidneys relative to WT UUO kidneys (Figure 3.7A-E) supporting the idea that *Trpc6*-deficiency is protective in this kidney disease model.

3.4 Expression profile of TRPC channels in the renal cortex

The genomic absence of one TRPC channel may affect the expression of the remaining ones, which could contribute to the renal outcome. qRT-PCR was performed to first identify the relative expression of TRPC family members (TRPC1-7) in the renal cortices of WT and *Trpc6*-deficient mice. In sham-operated kidneys, deletion of *Trpc6* was found to be associated with reduced *Trpc2*, *Trpc3* and *Trpc4* mRNA expression compared to WT kidneys (Figure 3.8A-D). Conversely, *Trpc6*-deficiency increased *Trpc1* mRNA expression. Similarly, *Trpc5* mRNA was present in *Trpc6*$^{-/-}$ kidneys but below the detection limit in WT kidneys (Figure 3.8E, Figure 3.9A). As reported earlier [34], whereas *Trpc6* mRNA expression could be determined in WT kidneys, it was below the detection levels in *Trpc6*$^{-/-}$ kidneys(Figure 3.8F).*Trpc7* mRNA was not detectable in both WT and *Trpc6*$^{-/-}$ kidneys, but was present in WT brain tissue, which served as a positive control (Figure 3.9B).

Next, it was determined whether in WT animals the relative expression of TRPC isoforms is affected by UUO. Interestingly, ureter obstruction did not affect the relative mRNA expression levels of most TRPC family members including *Trpc2*, *Trpc3*, *Trpc4*, and *Trpc5* (Figure 3.8B,C,D,E). In contrast, UUO provoked an approximately 50% downregulation of *Trpc1* and notably a 60% upregulation of *Trpc6* mRNA expression in WT kidneys (Figure 3.8A and F) relative to sham-operated WT animals.

Finally, the impact of *Trpc6*-deficiency on the relative TRPC-isoform expression profile in UUO kidneys was studied. Under these conditions, a highly significant decrease of *Trpc2* and *Trpc4* transcript levels was evident in the knockout kidneys (Figure 3.8B,D) whereas *Trpc1* and *Trpc3* mRNA levels remained stable compared to WT (Figure 3.8A,C). In

addition, *Trpc5* transcript levels were below detection levels in the presence and absence of *Trpc6* (Figure 3.8E), and as expected in *Trpc6*$^{-/-}$ kidneys lacking *Trpc6* mRNA (Figure 3.8F).

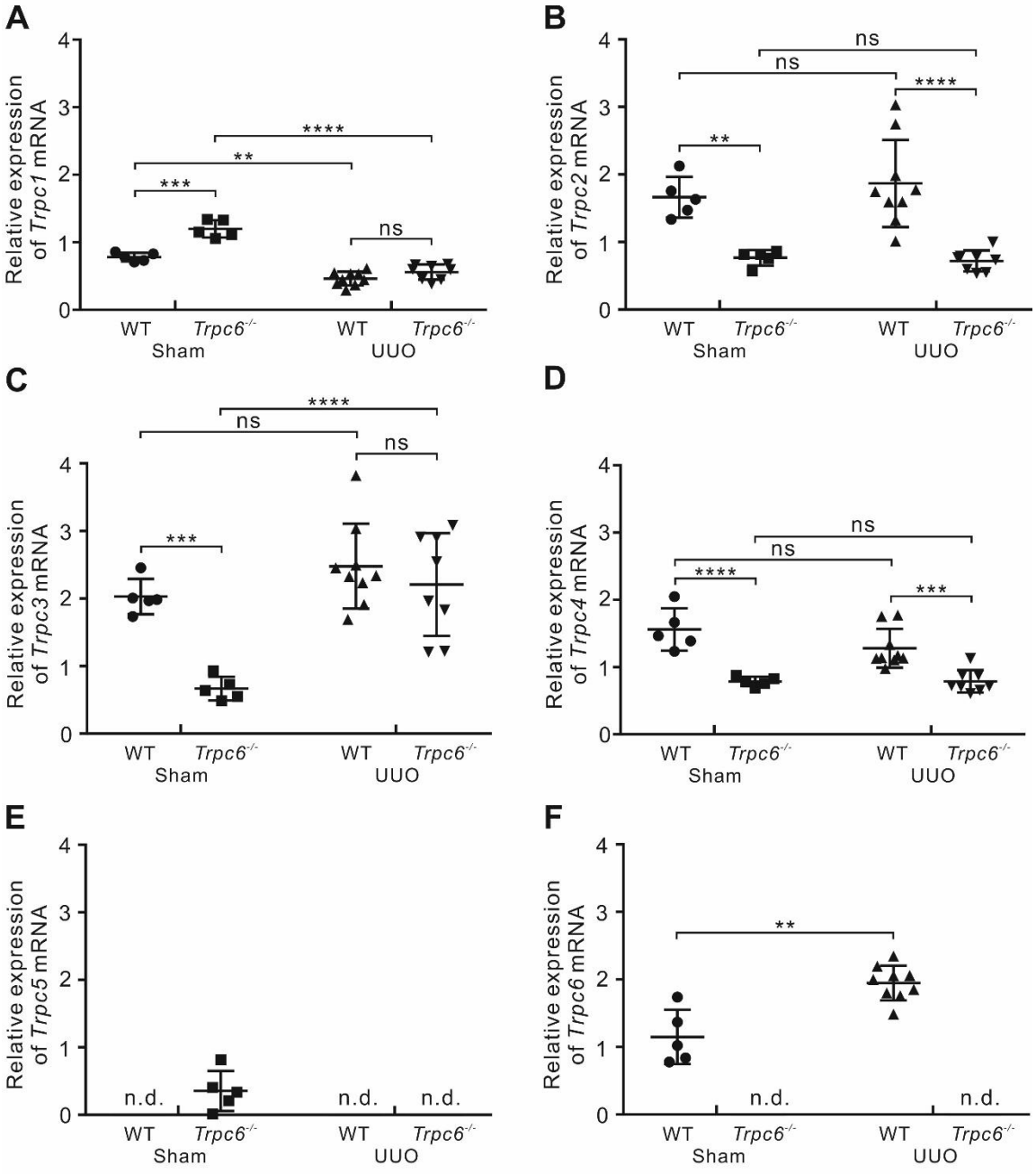

***Figure 3.8*: Expression of renal TRPC channels in wild-type (WT) and *Trpc6*$^{-/-}$ mice.** Renal mRNA levels of **(A)** transient receptor potential cation channel 1 (TRPC1), **(B)** TRPC2, **(C)** TRPC3, **(D)** TRPC4, **(E)** TRPC5 and **(F)** TRPC6 in sham-operated groups and in UUO-operated groups. Renal mRNA expression data were determined in n=5 each for sham-operated WT and *Trpc6*$^{-/-}$ mice, n=9 for UUO-operated WT mice and n=8 for UUO-operated *Trpc6*$^{-/-}$ mice. The relative standard curve method was used for relative quantification. All data are *means* ± *SD*., ns *p>0.05*, ***p<0.01*, ****p*<0.001, *****p*<0.0001. ns, *not significant*; n.d., *not detected.*

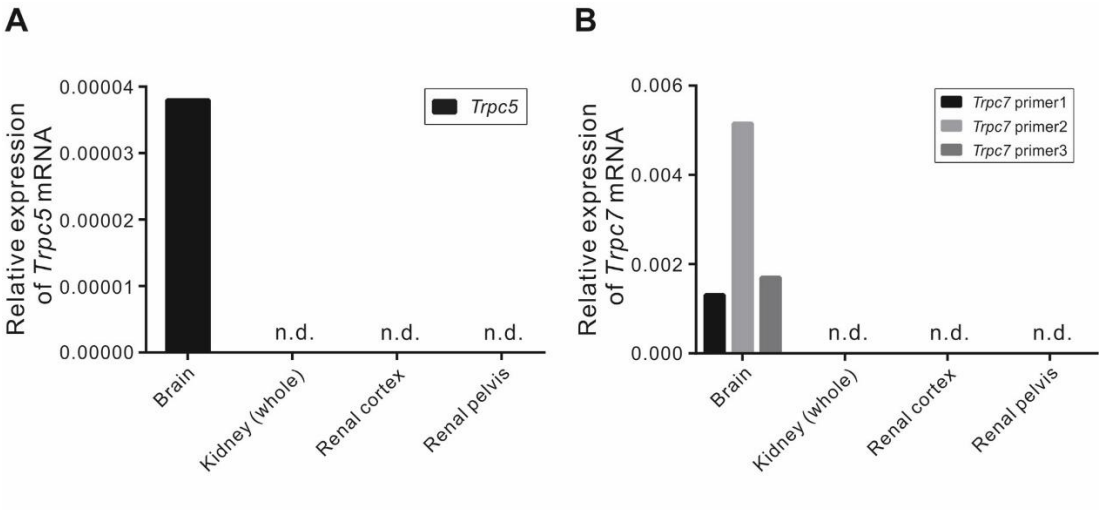

***Figure 3.9*: Expression of *Trpc5* and *Trpc7* mRNA in brain and kidney samples in wildtype (WT) mice.** (A) *Trpc5* mRNA expression and (B) *Trpc7* mRNA expression (detected by three primer pairs with different sequences). At mRNA level, *Trpc5* and *Trpc7* are highly expressed in brain but not in kidneys of WT mice. The ΔΔCT method was used for relative quantification. n.d., *not detected*.

3.5 UUO in NZO mice

Next, the complex disease NZO mouse model was used to evaluate UUO nephropathy and regulation of TRPC channel expression in an inbred obese mouse strain carrying susceptibility genes for diabetes and hypertension. In the NZO mice, UUO also caused significant damage to the kidney. Histological analyses showed that UUO induced increases in the PAS^+ area, $PCNA^+$ cells, SR^+ area, $F4/80^+$ area and $CD3^+$ cells (Figure 3.10). Furthermore, a UUO-induced increase was detected in mRNA expression of the pro-fibrotic markers Col1α1, Col3α1, Col4α1 and TGFβ1 (except αSMA) (Figure 3.11A) and the pro-inflammatory markers IL1β, IL6, TNFα, ICAM1, VCAM1 and MCP1 relative to the sham-operated group (Figure 3.11B).

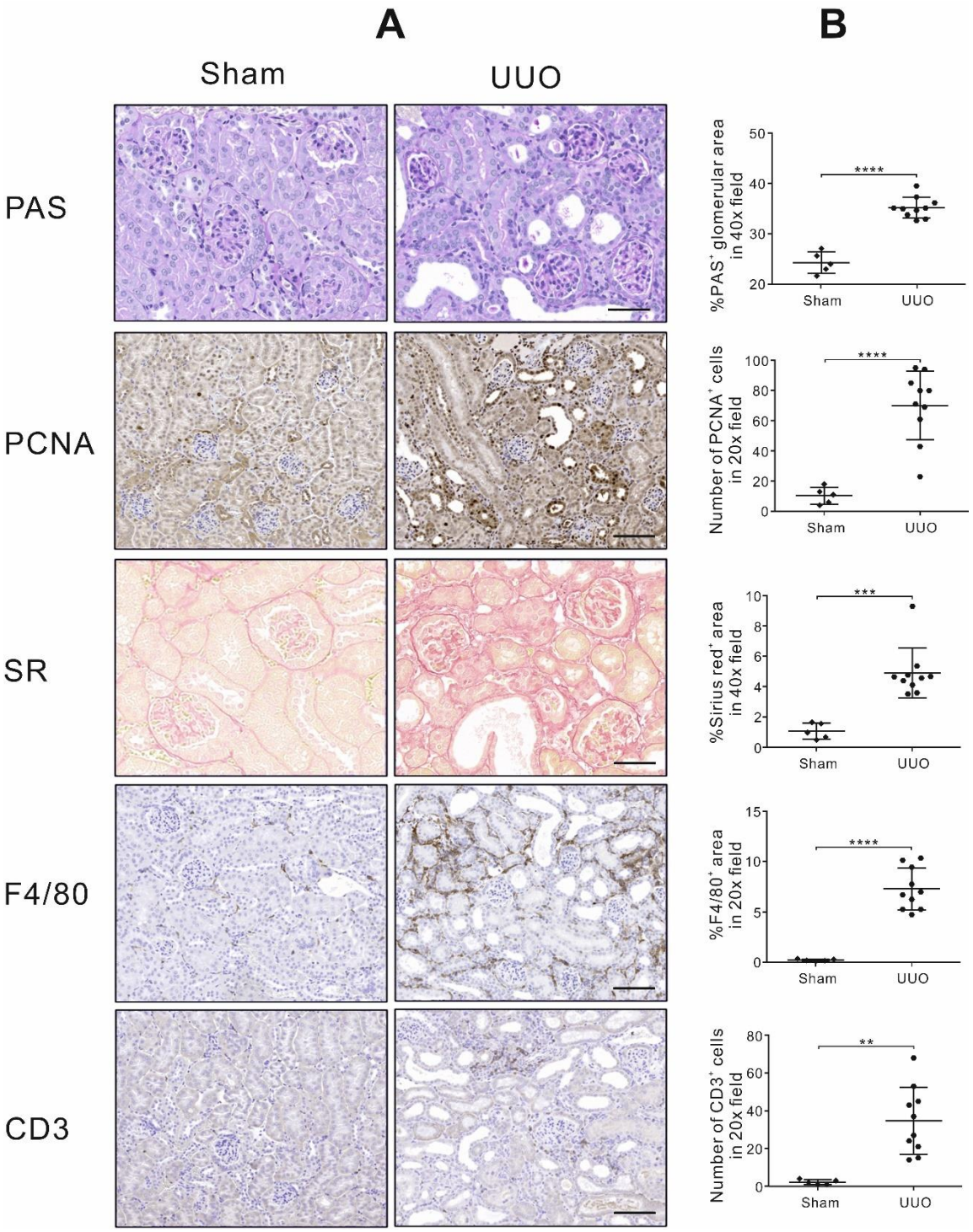

***Figure 3.10*: Markers of fibrosis and inflammation in *New Zealand obese* (NZO) mice. (A)** *Periodic acid Schiff* (PAS) stain: marker of glomerular damage (40x. Scale bar: 50 µm). Proliferating cell nuclear antigen (PCNA) antibody stain: marker of cell regeneration (20x. Scale bar: 100 µm). Sirius red (SR) stain: marker of interstitial fibrosis (40x. Scale bar: 50 µm). F4/80 antibody stain: macrophage marker (20x. Scale bar: 100 µm) and CD3 antibody stain: T-cell marker (20x. Scale bar: 100 µm) in sham-operated group and UUO-operated groups. **(B)** All quantification data are *means* ± *SD*. Data were determined in n=5 for sham-operated kidneys, n=10 for UUO-operated kidneys. ***p*<0.01, ****p*<0.001 and *****p*<0.0001, ns, *not significant*.

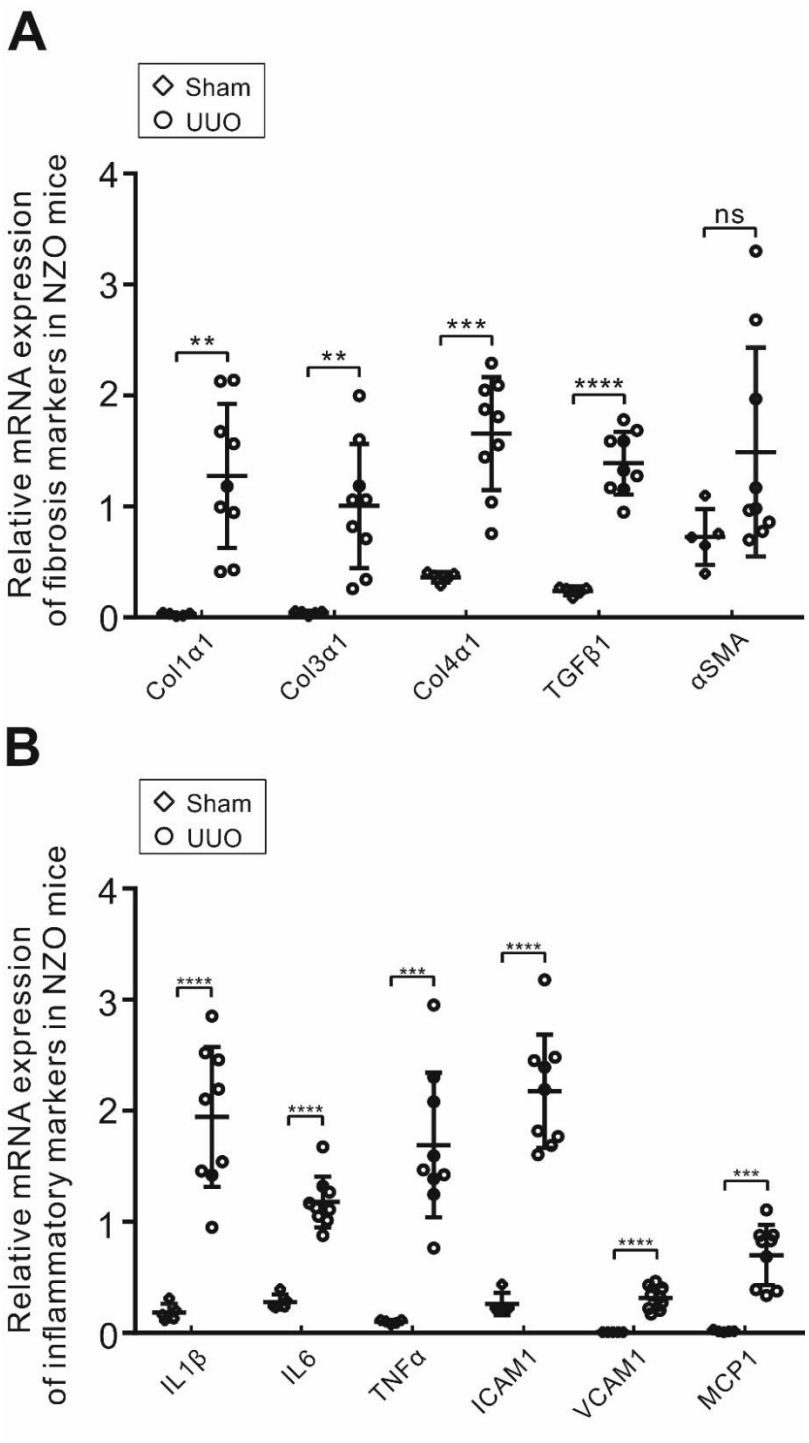

***Figure 3.11*: Expression of markers of fibrosis and inflammation in *New Zealand obese* (NZO) mice. (A)** Renal mRNA levels of fibrosis markers: collagen type 1, alpha 1 (Col1α1), collagen type 3, alpha 1 (Col3α1), collagen type 4, alpha 1 (Col4α1), transforming growth factor beta 1 (TGFβ1) and alpha smooth muscle actin (αSMA) in sham-operated group and in UUO-operated group. **(B)** Renal mRNA levels of inflammation markers: interleukin 1 beta (IL1β), interleukin 6 (IL6), tumor necrosis factor alpha (TNFα), intercellular adhesion molecule 1 (ICAM1), vascular cell adhesion molecule 1 (VCAM1) and monocyte chemotactic protein *1* (MCP1) in sham-operated group and UUO-operated groups. All mRNA expression data were determined in n=5 for sham-operated kidneys, n=9 for UUO-operated kidneys. The relative standard curve method was used for relative quantification. All data are means ± SD., ns *p>0.05*, ***p*<0.01, ****p*<0.001, *****p*<0.0001 and *****p*<0.0001. *ns, not significant*.

The relative expression profile of TRPC genes was also examined in kidneys of NZO mice in sham and UUO kidneys by qRT-PCR. NZO sham kidneys expressed mRNA of six TRPC genes in the renal cortex (Figure 3.12). UUO caused up-regulation of *Trpc6* mRNA expression while *Trpc1* and *Trpc5* mRNA expression was down-regulated. There was no change in *Trpc2* and *Trpc3* mRNA expression in NZO kidneys upon UUO surgery (Figure 3.12). It is noteworthy that *Trpc7* mRNA was not detectable in NZO kidneys without UUO or in response to UUO (Figure 3.12), which is in line with the findings in WT and *Trpc6*$^{-/-}$ kidneys (Figure 3.9).

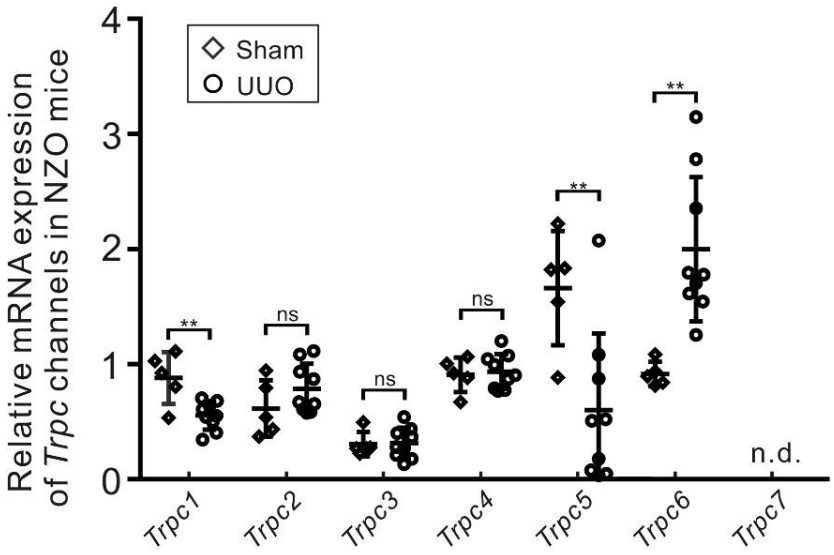

***Figure 3.12*: Expression of renal TRPC channels in *New Zealand obese* (NZO) mice.** Renal mRNA levels of TRPC1-7 channels in sham-operated group and in UUO-operated group. Renal mRNA expression data were determined in n=5 for sham-operated kidneys, n=9 for UUO-operated kidneys. The relative standard curve method was used for relative quantification. All data are *means* ± *SD*, ***p*<0.01, ns, *not significant.* n.d., *not detected*.

Chapter 4
Discussion

The major findings of the study are threefold. First, the findings provide evidence for a marked up-regulation of renal TRPC6 expression upon UUO in WT and NZO mice. This up-regulation is associated with renal fibrosis and immune cell infiltration in both mouse models. A striking reduction of fibrosis was observed after genomic deletion of TRPC6, which was associated with reduced immune cell infiltration. On a conceptual level, these findings are consistent with the idea that TRPC6 fulfills an important role in promoting renal fibrosis after UUO in mice. Second, the study further reveals an unrecognized down-regulation of *Trpc2* and *Trpc4* mRNA expression in *Trpc6*$^{-/-}$ sham and *Trpc6*$^{-/-}$ UUO kidneys compared to WT sham and WT UUO kidneys, respectively, which suggests that TRPC2/4 could also fulfill inhibitory functions in renal fibrosis, at least after genomic deletion of TRPC6. Third, a significant down-regulation of *Trpc1* and *Trpc5* mRNA levels was observed in UUO kidneys of NZO mice, which indicates that these genes could play an additional protective role in renal fibrosis and inflammation in a polygenic environment with susceptibility genes for obesity, diabetes and hypertension. Although most TRPC subunits can form functional homomeric channels, heteromerization of TRPC channel subunits of either the same subfamily or different subfamilies has been widely observed and may extend the functional diversity of the TRPC channel family in progressive kidney diseases.

4.1 TRPC6 in the kidney

The structural and functional defects of the glomerular filtration barrier are central mechanisms of proteinuric kidney disease. TRPC6, which is regarded as a key molecule of the slit-diaphragm, can be increasingly detected in various kidney diseases such as FSGS [56; 57], diabetic nephropathy [42; 58; 59; 60], minimal change nephrosis [57; 61] and membranous nephropathy [61; 62; 63]. Recent studies show that genomic inhibition of TRPC6 can reduce rat kidney fibroblast proliferation and myofibroblast differentiation *in vitro* and thereby diminishes renal fibrosis in the UUO model [34; 38]. In the present study, UUO surgery was carried out to induce early stage CKD; however, three different

mouse strains were used: WT, *Trpc6*$^{-/-}$ and NZO mice. By performing such experiments, an effort was made to evaluate the therapeutic efficiency of genomic TRPC6 inhibition in obstructive nephropathy in the UUO model and to determine the effect of TRPC6 ablation and UUO on the expression of all seven TRPC channels in the kidneys of the three different genotypes. In line with previous findings, the data show that genomic deletion of TRPC6 is associated with a reduction of renal fibrosis in the UUO mouse model. In addition, TRPC6-deletion is also associated with less inflammatory cell infiltration in UUO kidneys. It is further revealed that TRPC6-deficiency *per se* impacts on renal TRPC channel expression in mice as indicated by reduced mRNA expression of TRPC2, TRPC3 and TRPC4 and increased mRNA expression of TRPC1. Moreover, UUO is found to cause reduced *Trpc1* mRNA and increased *Trpc6* mRNA expression without changes of *Trpc3* expression in WT kidneys and also in the kidneys of NZO mice. Collectively, the data suggest that counterbalanced or increased expression of TRPC1 and TRPC6 could play a role in UUO-induced kidney damage. Since genomic deletion of *Trpc6* improved renal fibrosis and was associated with an increase of *Trpc1* mRNA expression and a reduction of *Trpc2* and *Trpc4* mRNA expression to levels similar or even greater than those observed in WT UUO/sham-operated kidneys, it can be concluded that TRPC6 could drive renal fibrosis with or without modifying effects of TRPC1/2/4.

4.2 TRPC6 and TRPC3

Of note, the data in the present study show that the deficiency of TRPC6 is associated with reduced *Trpc3* mRNA expression in *Trpc6*$^{-/-}$ kidneys compared to WT kidneys, which disappears in obstructive nephropathy. At first glance, this is surprising as it was observed in a previous publication on *Trpc6*$^{-/-}$ mice that loss of TRPC6 is associated with up-regulation of constitutively active TRPC3-type channels in some arteries [50]. However, according to present knowledge, TRPC channel (TRPC1-7) expression and resulting putative (functional) counterbalancing effects have not been investigated in experimental obstructive nephropathy. This is of particular interest for TRPC3, which is capable of contributing to fibrogenesis and tissue inflammation [37; 64; 65; 66; 67]. Additionally, Wu et al. reported that TRPC3 mRNA expression is upregulated in UUO-induced renal fibrosis in both WT and *Trpc6*$^{-/-}$ mice[34]. However, the present data do not show an increase in TRPC3 expression level in WT kidneys (or in the NZO mouse model), which

is an argument against it playing an important role in the progression of fibrosis in obstructive nephropathy. Based on the findings, it is unlikely that increased TRPC3 expression upon UUO accounts for the beneficial role of TRPC6-deficiency in this model of kidney failure. These mechanisms might be particularly relevant for inherited FSGS caused by mutations in TRPC6 [21; 68]. This conclusion is supported by the findings demonstrating that knockout of both TRPC3 and TRPC6 did not diminish UUO-induced fibrosis more than deletion of TRPC6 alone [34]. BTP2, an inhibitor of several TRPC channels, including TRPC3 and TRPC6, had an effect similar to that of *Trpc6* knockout on fibrosis, but also attenuated the up-regulation of TRPC6 expression, which suggests that TRPC6 channel activity may induce its own gene expression in the UUO model [5] and promote fibrosis in this model. Nevertheless, future studies using more specific TRPC3/6 blockers are necessary to clarify the contribution of TRPC3 in the absence and presence of functional TRPC6 channels. Recently, novel TRPC6 blockers have been developed [69; 70; 71], and these could represent important tools for evaluating the role of TRPC6 under these conditions.

4.3 TRPC6 and TRPC5

Whether TRPC5 activity mediates FSGS onset and progression is unknown. Recently, Zhou et al. identified a small molecule, AC1903, which specifically blocks TRPC5 channel activity in glomeruli of proteinuric rats [44]. Chronic administration of AC1903 suppressed severe proteinuria and prevented podocyte loss in a transgenic rat model of FSGS. AC1903 also provided therapeutic benefit in a rat model of hypertensive proteinuric kidney disease [44]. Their data indicate that TRPC5 activity drives kidney disease and that TRPC5 inhibitors may be valuable for the treatment of progressive proteinuric kidney diseases. The present study reveals a previously unrecognized renal counter-regulation of TRPC5 and TRPC7 gene expression, which paralleled the increased expression of TRPC6 at mRNA levels in UUO kidneys of NZO mice. It is possible that this counter-regulation represents an intrinsic mechanism to delay TRPC6-driven renal fibrosis and inflammation in a genetic context/background (NZO/HIBomDife) carrying susceptibility genes for obesity, diabetes and hypertension. This conclusion is supported by findings that TRPC5 is not expressed in normal kidneys of mice [72], but in kidneys of rats [44; 73; 74]. Further experimental means (i.e. podocyte isolation, Western-Blot, etc.) should be

applied to examine detailed TPRC5 expression. Future studies should also evaluate the potential of specific drug targeting of TRPC5 under these conditions. Based on the expression data, it is expected that specific TRPC5 inhibition is of little value for limiting progressive kidney disease in *Trpc6*-deficiency, which might have important implications for treatment options in human FSGS caused by loss-of-function TRPC6 mutations [68]. Nevertheless, future studies are necessary to test and clarify the role of pharmacological TRPC5 targeting by agonists and antagonists under these conditions.

While most TRPC isoforms can form functional homomeric or heteromeric TRPC channels, and even include TRP isoforms from different subfamilies, the above documented up- or down-regulation of the individual TRPC channels may cause functional diversity of the various TRPCs in the process of fibrosis and inflammation in UUO kidneys. Additional diversification might be caused by the various cell types with the individual TRPC channel subunits, which extend functional diversity and are assumed to affect the outcome. Therefore, there is an urgent need to test the potency of specific pharmacological TRPC modulators, e.g. TRPC6 blockers and TRPC1 agonists, to reveal the contribution of the individual TRPC channel subfamilies to the progression of chronic kidney disease.

4.4 Renal fibrosis and inflammation

Mechanisms that promote kidney disease progression include renal atrophy, fibrosis and increased leukocyte infiltration into the kidneys [75; 76]. Renal fibrosis and inflammation are two histological hallmarks of progressive kidney disease and specific antibody staining is a common tool for estimating renal damage [77; 78]. It is tempting to speculate that a similar process is involved in UUO, which contributes to fibrosis and chronic kidney failure [48].In previous studies, TRPC6 was reported to contribute to fibroblast-to-myofibroblast transdifferentiation (FMT) and is thought to promote tissue scarring [79; 80; 81]. Recent research shows that TRPC6 is involved in the pathogenesis of kidney fibrosis and that genomic inhibition of TRPC6 can ameliorate renal fibrosis [34; 38]. TRPC6 is a member of non-selective cation channels, indicating that increased Ca^{2+} flux could be one of the pathogenetic factors in myo-/fibroblasts [82]. This study found that *Trpc6* loss reduced the renal fibrosis in the murine UUO model. In addition, it could be shown that

TRPC6-deficiency caused a decreased mRNA expression of multiple pro-fibrotic genes. These results therefore confirm the previous finding that *Trpc6* deletion attenuates UUO-induced kidney fibrosis in mice [34].

The renal damage occurring in CKD is, at least in part, promoted by the immune system [83]. Most kidney diseases involve an accumulation of immune cells of the innate immune system (e.g. macrophages and neutrophils) and of the adaptive immune system (e.g. T cells). In particular, tubulointerstitial monocyte immune infiltration can mediate tissue remodeling that ultimately promotes fibrogenesis, renal atrophy and thus kidney failure [84; 85; 86]. Until now, no putative immunoregulatory role of TRPC6 has been reported in obstructive nephropathy. In the present study, the results of histological analyses show a reduction of the inflammatory cell infiltration in *Trpc6*$^{-/-}$ kidneys compared with WT kidneys after UUO. It is noteworthy that UUO provoked an increase in mRNA expression of the pro-inflammatory markers in both *Trpc6*$^{-/-}$ and WT kidneys. However, a significant beneficial effect of the *Trpc6*-knockout was not found on the expression of pro-inflammatory markers at the mRNA level upon UUO surgery. Taken together, these data point to a complex (in-)direct contribution of TRPC6 to renal inflammation in the UUO model.

To estimate renal apoptosis as well as regenerative potential, kidney sections were stained with antibodies against the apoptosis marker cleaved-caspase 3 (cCasp3) and the mitosis marker proliferating cell nuclear antigen (PCNA). Since cCasp3 and PCNA levels correlate positively with renal injury, they are commonly used to determine the degree of renal damage under chronic damaging conditions [87; 88; 89]. It is known that chronic activation of TRPC6 is positively correlated with the rate of apoptosis in cells such as podocytes [90; 91] and endothelial cells [92]. In this study, a reduction of cCasp3^{+} cells is observed in *Trpc6*$^{-/-}$ UUO kidneys. It might also reflect less inflammatory cell infiltration in the kidneys of *Trpc6*$^{-/-}$ mice. PCNA is known as a probe for the detection of cell proliferative activity[93]. PCNA^{+} cells in the present study were found to be increased after UUO in both WT and *Trpc6*$^{-/-}$ kidneys. Nevertheless, there was no significant difference in PCNA^{+} cells between WT and *Trpc6*$^{-/-}$ mice. Correlated with the result of cCasp3 cell infiltration, it might be due to an imbalance between cell apoptosis and proliferative activity, or it might be because PCNA is also regulated by other factors, e.g.

p53[94] and DNA damage binding protein 2 (DDB2)[95]. In short, the results indicate that TRPC6-deficiency protects renal cells from UUO-induced apoptosis.

4.5 Diabetic nephropathy

Nowadays, 25-40% of diabetic patients suffer from diabetic nephropathy [96; 97]. Thus, diabetic patients can be considered high-risk patients for the development of chronic kidney disease. Diabetic nephropathy shows pronounced glomerular changes that are present in patients with long-standing diabetes often even before the detection of albumin in the urine. Several mechanisms that can lead to diabetic nephropathy are under discussion. It has been evaluated whether a UUO-operated NZO mouse model could represent a model of progressive nephropathy in co-morbid conditions of obesity, hypertension and type 2 diabetes [46], which had not been reported before. Present results show that UUO can successfully induce renal fibrosis and inflammatory infiltration in the NZO mouse model (NZO/HIBomDife) carrying susceptibility genes for obesity, diabetes and hypertension. This study also suggests that changed expression of TRPC channels, specifically TRPC1, TRPC5 and TRPC6, could be involved in this process. The results suggest that the UUO-operated NZO mouse model might be a valuable mouse model for use in evaluating the specific contribution of TRPC6 and other TRPC channel subfamilies to renal injury in individuals with obesity, hypertension and diabetes. This approach could benefit from better testing, i.e. TRPC subfamily specific blockers and agonists. Due to recent progress in this field [44; 69; 70; 71], it is to be hoped that such drugs will be available in the near future for *in vivo* testing.

Chapter 5
Conclusions and Future Directions

In this study, it was observed for the first time that inhibition of TRPC6 is associated with a decrease in inflammatory cell infiltration in the murine UUO model. Also, the findings of this study are in line with the concept that up-regulation of TRPC6 contributes to fibrosis in UUO kidneys, which supports the view that increased TRPC6 expression can play an important pathophysiological role in the development of progressive kidney disease [32; 57; 98; 99]. Moreover, the present results imply that the genomic loss of TRPC6 is associated with dysregulation of multiple TRPC channels (TRPC1-4) under chronic kidney damaging conditions, which could represent additional drivers of renal fibrosis and chronic kidney disease. The results show that UUO also causes up-regulation of TRPC6 in kidneys of NZO mice, which implies that inhibition of TRPC6 is also a promising therapeutic strategy for the treatment of renal fibrosis and immune cell infiltration in polygenic models for human metabolic syndrome and type 2 diabetes.

Further studies are required to demonstrate the complex role of TRPC6 in the progression of renal insufficiency, from AKI to CKD and ESRD. Meanwhile, studies are needed to confirm whether TRPC6 has the same effects on renal insufficiency based on different causes, e.g. diabetic nephropathy, hypertensive nephropathy and glomerulonephritis. Thus, more kidney models and animal strains could be taken into consideration. It might also be interesting to see whether the effects of TRPC6-specific blockers may differ from those of global inhibition of TRPC6 by gene knockout. With regard to future drug treatment of kidney diseases, the further studies would be the important theoretical basis for the discovery of drugs with tolerable TRPC6-specific blockers, i.e. TRPC6-blocking drugs without overt adverse effects for patients.

Chapter 6
References / Literaturverzeichnis

[1] A. Levin, M. Tonelli, J. Bonventre, J. Coresh, J.A. Donner, A.B. Fogo, C.S. Fox, R.T. Gansevoort, H.J.L. Heerspink, M. Jardine, B. Kasiske, A. Kottgen, M. Kretzler, A.S. Levey, V.A. Luyckx, R. Mehta, O. Moe, G. Obrador, N. Pannu, C.R. Parikh, V. Perkovic, C. Pollock, P. Stenvinkel, K.R. Tuttle, D.C. Wheeler, K.U. Eckardt, and I.S.N.G.K.H.S. participants, Global kidney health 2017 and beyond: a roadmap for closing gaps in care, research, and policy. Lancet 390 (2017) 1888-1917.

[2] G.B.D. Mortality, and C. Causes of Death, Global, regional, and national life expectancy, all-cause mortality, and cause-specific mortality for 249 causes of death, 1980-2015: a systematic analysis for the Global Burden of Disease Study 2015. Lancet 388 (2016) 1459-1544.

[3] A.C. Webster, E.V. Nagler, R.L. Morton, and P. Masson, Chronic Kidney Disease. Lancet 389 (2017) 1238-1252.

[4] A.B. Farris, and R.B. Colvin, Renal interstitial fibrosis: mechanisms and evaluation. Curr Opin Nephrol Hypertens 21 (2012) 289-300.

[5] J. Schlondorff, TRPC6 and kidney disease: sclerosing more than just glomeruli? Kidney Int 91 (2017) 773-775.

[6] A.A. Eddy, Overview of the cellular and molecular basis of kidney fibrosis. Kidney Int Suppl (2011) 4 (2014) 2-8.

[7] P. Romagnani, G. Remuzzi, R. Glassock, A. Levin, K.J. Jager, M. Tonelli, Z. Massy, C. Wanner, and H.J. Anders, Chronic kidney disease. Nat Rev Dis Primers 3 (2017) 17088.

[8] A.V. Kshirsagar, M.S. Joy, S.L. Hogan, R.J. Falk, and R.E. Colindres, Effect of ACE inhibitors in diabetic and nondiabetic chronic renal disease: a systematic overview of randomized placebo-controlled trials. Am J Kidney Dis 35 (2000) 695-707.

[9] B. Thomas, K. Matsushita, K.H. Abate, Z. Al-Aly, J. Arnlov, K. Asayama, R. Atkins, A. Badawi, S.H. Ballew, A. Banerjee, L. Barregard, E. Barrett-Connor, S. Basu, A.K. Bello, I. Bensenor, J. Bergstrom, B. Bikbov, C. Blosser, H. Brenner, J.J. Carrero, S. Chadban, M. Cirillo, M. Cortinovis, K. Courville, L. Dandona, R. Dandona, K. Estep, J. Fernandes, F. Fischer, C. Fox, R.T. Gansevoort, P.N. Gona, O.M. Gutierrez, S. Hamidi, S.W. Hanson, J. Himmelfarb, S.K. Jassal, S.H. Jee, V. Jha,

A. Jimenez-Corona, J.B. Jonas, A.P. Kengne, Y. Khader, Y.H. Khang, Y.J. Kim, B. Klein, R. Klein, Y. Kokubo, D. Kolte, K. Lee, A.S. Levey, Y. Li, P. Lotufo, H.M.A. El Razek, W. Mendoza, H. Metoki, Y. Mok, I. Muraki, P.M. Muntner, H. Noda, T. Ohkubo, A. Ortiz, N. Perico, K. Polkinghorne, R. Al-Radaddi, G. Remuzzi, G. Roth, D. Rothenbacher, M. Satoh, K.U. Saum, M. Sawhney, B. Schottker, A. Shankar, M. Shlipak, D.A.S. Silva, H. Toyoshima, K. Ukwaja, M. Umesawa, S.E. Vollset, D.G. Warnock, A. Werdecker, K. Yamagishi, Y. Yano, N. Yonemoto, M.E.S. Zaki, M. Naghavi, M.H. Forouzanfar, C.J.L. Murray, J. Coresh, T. Vos, G.F.R.C. Global Burden of Disease, C.K.D.P. Consortium, and G. Global Burden of Disease Genitourinary Expert, Global Cardiovascular and Renal Outcomes of Reduced GFR. J Am Soc Nephrol 28 (2017) 2167-2179.

[10] P. Rossignol, R. Agarwal, B. Canaud, A. Charney, G. Chatellier, J.C. Craig, W.C. Cushman, R.T. Gansevoort, B. Fellstrom, D. Garza, N. Guzman, F.A. Holtkamp, G.M. London, Z.A. Massy, A. Mebazaa, P.G.M. Mol, M.A. Pfeffer, Y. Rosenberg, L.M. Ruilope, J. Seltzer, A.M. Shah, S. Shah, B. Singh, B.V. Stefansson, N. Stockbridge, W.G. Stough, K. Thygesen, M. Walsh, C. Wanner, D.G. Warnock, C.S. Wilcox, J. Wittes, B. Pitt, A. Thompson, and F. Zannad, Cardiovascular outcome trials in patients with chronic kidney disease: challenges associated with selection of patients and endpoints. Eur Heart J (2017).

[11] X. Xu, X. Qin, Y. Li, D. Sun, J. Wang, M. Liang, B. Wang, Y. Huo, F.F. Hou, and T. investigators of the Renal Substudy of the China Stroke Primary Prevention, Efficacy of Folic Acid Therapy on the Progression of Chronic Kidney Disease: The Renal Substudy of the China Stroke Primary Prevention Trial. JAMA Intern Med 176 (2016) 1443-1450.

[12] C. Baigent, M.J. Landray, C. Reith, J. Emberson, D.C. Wheeler, C. Tomson, C. Wanner, V. Krane, A. Cass, J. Craig, B. Neal, L. Jiang, L.S. Hooi, A. Levin, L. Agodoa, M. Gaziano, B. Kasiske, R. Walker, Z.A. Massy, B. Feldt-Rasmussen, U. Krairittichai, V. Ophascharoensuk, B. Fellstrom, H. Holdaas, V. Tesar, A. Wiecek, D. Grobbee, D. de Zeeuw, C. Gronhagen-Riska, T. Dasgupta, D. Lewis, W. Herrington, M. Mafham, W. Majoni, K. Wallendszus, R. Grimm, T. Pedersen, J. Tobert, J. Armitage, A. Baxter, C. Bray, Y. Chen, Z. Chen, M. Hill, C. Knott, S. Parish, D. Simpson, P. Sleight, A. Young, R. Collins, and S. Investigators, The effects of lowering LDL cholesterol with simvastatin plus ezetimibe in patients with chronic kidney disease (Study of Heart and Renal Protection): a randomised placebo-

controlled trial. Lancet 377 (2011) 2181-92.

[13] D.E. Clapham, C. Montell, G. Schultz, and D. Julius, International Union of Pharmacology. XLIII. Compendium of voltage-gated ion channels: transient receptor potential channels. Pharmacol Rev 55 (2003) 591-6.

[14] C. Montell, and G.M. Rubin, Molecular characterization of the Drosophila trp locus: a putative integral membrane protein required for phototransduction. Neuron 2 (1989) 1313-23.

[15] F. Wong, E.L. Schaefer, B.C. Roop, J.N. LaMendola, D. Johnson-Seaton, and D. Shao, Proper function of the Drosophila trp gene product during pupal development is important for normal visual transduction in the adult. Neuron 3 (1989) 81-94.

[16] Z. Yue, J. Xie, A.S. Yu, J. Stock, J. Du, and L. Yue, Role of TRP channels in the cardiovascular system. Am J Physiol Heart Circ Physiol 308 (2015) H157-82.

[17] S.F. Pedersen, G. Owsianik, and B. Nilius, TRP channels: an overview. Cell Calcium 38 (2005) 233-52.

[18] K. Venkatachalam, and C. Montell, TRP channels. Annu Rev Biochem 76 (2007) 387-417.

[19] I.S. Ramsey, M. Delling, and D.E. Clapham, An introduction to TRP channels. Annu Rev Physiol 68 (2006) 619-47.

[20] M. Riehle, D. Tsvetkov, B.O. Gohlke, R. Preissner, C. Harteneck, M. Gollasch, and B. Nurnberg, Molecular basis for the sensitivity of TRP channels to polyunsaturated fatty acids. Naunyn Schmiedebergs Arch Pharmacol (2018).

[21] L. Marko, M. Mannaa, T.N. Haschler, S. Kramer, and M. Gollasch, Renoprotection: focus on TRPV1, TRPV4, TRPC6 and TRPM2. Acta Physiol (Oxf) 219 (2017) 589-612.

[22] J.C. Gonzalez-Cobos, and M. Trebak, TRPC channels in smooth muscle cells. Front Biosci (Landmark Ed) 15 (2010) 1023-39.

[23] G. Vazquez, B.J. Wedel, O. Aziz, M. Trebak, and J.W. Putney, Jr., The mammalian TRPC cation channels. Biochim Biophys Acta 1742 (2004) 21-36.

[24] M. Trebak, G. Vazquez, G.S. Bird, and J.W. Putney, Jr., The TRPC3/6/7 subfamily of cation channels. Cell Calcium 33 (2003) 451-61.

[25] C. Strubing, G. Krapivinsky, L. Krapivinsky, and D.E. Clapham, TRPC1 and TRPC5 form a novel cation channel in mammalian brain. Neuron 29 (2001) 645-55.

[26] T. Hofmann, M. Schaefer, G. Schultz, and T. Gudermann, Subunit composition of

mammalian transient receptor potential channels in living cells. Proc Natl Acad Sci U S A 99 (2002) 7461-6.

[27] U. Storch, A.L. Forst, M. Philipp, T. Gudermann, and M. Mederos y Schnitzler, Transient receptor potential channel 1 (TRPC1) reduces calcium permeability in heteromeric channel complexes. J Biol Chem 287 (2012) 3530-40.

[28] J. Kim, M. Kwak, J.P. Jeon, J. Myeong, J. Wie, C. Hong, S.Y. Kim, J.H. Jeon, H.J. Kim, and I. So, Isoform- and receptor-specific channel property of canonical transient receptor potential (TRPC)1/4 channels. Pflugers Arch 466 (2014) 491-504.

[29] J.S. Woo, K.J. Lee, M. Huang, C.H. Cho, and E.H. Lee, Heteromeric TRPC3 with TRPC1 formed via its ankyrin repeats regulates the resting cytosolic Ca2+ levels in skeletal muscle. Biochem Biophys Res Commun 446 (2014) 454-9.

[30] H.N. Rubaiy, M.J. Ludlow, M. Henrot, H.J. Gaunt, K. Miteva, S.Y. Cheung, Y. Tanahashi, N. Hamzah, K.E. Musialowski, N.M. Blythe, H.L. Appleby, M.A. Bailey, L. McKeown, R. Taylor, R. Foster, H. Waldmann, P. Nussbaumer, M. Christmann, R.S. Bon, K. Muraki, and D.J. Beech, Picomolar, selective, and subtype-specific small-molecule inhibition of TRPC1/4/5 channels. J Biol Chem 292 (2017) 8158-8173.

[31] R. Ma, S. Chaudhari, and W. Li, Canonical Transient Receptor Potential 6 Channel: A New Target of Reactive Oxygen Species in Renal Physiology and Pathology. Antioxid Redox Signal 25 (2016) 732-748.

[32] D.V. Ilatovskaya, and A. Staruschenko, TRPC6 channel as an emerging determinant of the podocyte injury susceptibility in kidney diseases. Am J Physiol Renal Physiol 309 (2015) F393-7.

[33] S. Dogra, and F. Kaskel, Steroid-resistant nephrotic syndrome: a persistent challenge for pediatric nephrology. Pediatr Nephrol 32 (2017) 965-974.

[34] Y.L. Wu, J. Xie, S.W. An, N. Oliver, N.X. Barrezueta, M.H. Lin, L. Birnbaumer, and C.L. Huang, Inhibition of TRPC6 channels ameliorates renal fibrosis and contributes to renal protection by soluble klotho. Kidney Int 91 (2017) 830-841.

[35] D.V. Ilatovskaya, O. Palygin, V. Chubinskiy-Nadezhdin, Y.A. Negulyaev, R. Ma, L. Birnbaumer, and A. Staruschenko, Angiotensin II has acute effects on TRPC6 channels in podocytes of freshly isolated glomeruli. Kidney Int 86 (2014) 506-14.

[36] H. Huang, Y. You, X. Lin, C. Tang, X. Gu, M. Huang, Y. Qin, J. Tan, and F. Huang, Inhibition of TRPC6 Signal Pathway Alleviates Podocyte Injury Induced by TGF-

beta1. Cell Physiol Biochem 41 (2017) 163-172.

[37] Y. Saliba, R. Karam, V. Smayra, G. Aftimos, J. Abramowitz, L. Birnbaumer, and N. Fares, Evidence of a Role for Fibroblast Transient Receptor Potential Canonical 3 Ca2+ Channel in Renal Fibrosis. J Am Soc Nephrol 26 (2015) 1855-76.

[38] E.Y. Kim, P. Yazdizadeh Shotorbani, and S.E. Dryer, Trpc6 inactivation confers protection in a model of severe nephrosis in rats. J Mol Med (Berl) 96 (2018) 631-644.

[39] D. Zhang, B.I. Freedman, M. Flekac, E. Santos, P.J. Hicks, D.W. Bowden, S. Efendic, K. Brismar, and H.F. Gu, Evaluation of genetic association and expression reduction of TRPC1 in the development of diabetic nephropathy. Am J Nephrol 29 (2009) 244-51.

[40] S. Graham, Y. Gorin, H.E. Abboud, M. Ding, D.Y. Lee, H. Shi, Y. Ding, and R. Ma, Abundance of TRPC6 protein in glomerular mesangial cells is decreased by ROS and PKC in diabetes. Am J Physiol Cell Physiol 301 (2011) C304-15.

[41] X. Zhang, Z. Song, Y. Guo, and M. Zhou, The novel role of TRPC6 in vitamin D ameliorating podocyte injury in STZ-induced diabetic rats. Mol Cell Biochem 399 (2015) 155-65.

[42] R. Ma, L. Liu, W. Jiang, Y. Yu, and H. Song, FK506 ameliorates podocyte injury in type 2 diabetic nephropathy by down-regulating TRPC6 and NFAT expression. Int J Clin Exp Pathol 8 (2015) 14063-74.

[43] D. Spires, D.V. Ilatovskaya, V. Levchenko, P.E. North, A.M. Geurts, O. Palygin, and A. Staruschenko, The protective role of Trpc6 knockout in the progression of diabetic kidney disease. Am J Physiol Renal Physiol (2018).

[44] Y. Zhou, P. Castonguay, E.H. Sidhom, A.R. Clark, M. Dvela-Levitt, S. Kim, J. Sieber, N. Wieder, J.Y. Jung, S. Andreeva, J. Reichardt, F. Dubois, S.C. Hoffmann, J.M. Basgen, M.S. Montesinos, A. Weins, A.C. Johnson, E.S. Lander, M.R. Garrett, C.R. Hopkins, and A. Greka, A small-molecule inhibitor of TRPC5 ion channels suppresses progressive kidney disease in animal models. Science 358 (2017) 1332-1336.

[45] G. Fesus, G. Dubrovska, K. Gorzelniak, R. Kluge, Y. Huang, F.C. Luft, and M. Gollasch, Adiponectin is a novel humoral vasodilator. Cardiovasc Res 75 (2007) 719-27.

[46] F. Mirhashemi, S. Scherneck, O. Kluth, D. Kaiser, H. Vogel, R. Kluge, A. Schurmann, S. Neschen, and H.G. Joost, Diet dependence of diabetes in the New Zealand

Obese (NZO) mouse: total fat, but not fat quality or sucrose accelerates and aggravates diabetes. Exp Clin Endocrinol Diabetes 119 (2011) 167-71.

[47] O. Zavaritskaya, N. Zhuravleva, J. Schleifenbaum, T. Gloe, L. Devermann, R. Kluge, M. Mladenov, M. Frey, H. Gagov, G. Fesus, M. Gollasch, and R. Schubert, Role of KCNQ channels in skeletal muscle arteries and periadventitial vascular dysfunction. Hypertension 61 (2013) 151-9.

[48] R.L. Chevalier, M.S. Forbes, and B.A. Thornhill, Ureteral obstruction as a model of renal interstitial fibrosis and obstructive nephropathy. Kidney Int 75 (2009) 1145-52.

[49] H.G. Joost, and A. Schurmann, The genetic basis of obesity-associated type 2 diabetes (diabesity) in polygenic mouse models. Mamm Genome 25 (2014) 401-12.

[50] A. Dietrich, Y.S.M. Mederos, M. Gollasch, V. Gross, U. Storch, G. Dubrovska, M. Obst, E. Yildirim, B. Salanova, H. Kalwa, K. Essin, O. Pinkenburg, F.C. Luft, T. Gudermann, and L. Birnbaumer, Increased vascular smooth muscle contractility in TRPC6-/- mice. Mol Cell Biol 25 (2005) 6980-9.

[51] L.J. Ma, H. Yang, A. Gaspert, G. Carlesso, M.M. Barty, J.M. Davidson, D. Sheppard, and A.B. Fogo, Transforming growth factor-beta-dependent and -independent pathways of induction of tubulointerstitial fibrosis in beta6(-/-) mice. Am J Pathol 163 (2003) 1261-73.

[52] Federation for Laboratory Animal Science Associations [Internet]. Guidelines - Recommendations - Felasa [cited 2018 Nov.]. Available from: http://www.felasa.eu/recommendations/guidelines/

[53] Gesellschaft für Versuchstierkunde [Internet]. GV-SOLAS [cited 2018 Nov.]. Available from: http://www.gv-solas.de/index.php?id=7

[54] American Physiological Society [Internet]. Guiding Principles for the Care and Use of Vertebrate Animals in Research and Training [cited 2018 Nov.]. Available from: http://www.the-aps.org/mm/SciencePolicy/About/Policy-Statements/Guiding-Principles.html

[55] L. Marko, E. Vigolo, C. Hinze, J.K. Park, G. Roel, A. Balogh, M. Choi, A. Wubken, J. Cording, I.E. Blasig, F.C. Luft, C. Scheidereit, K.M. Schmidt-Ott, R. Schmidt-Ullrich, and D.N. Muller, Tubular Epithelial NF-kappaB Activity Regulates Ischemic AKI. J Am Soc Nephrol 27 (2016) 2658-69.

[56] M.P. Winn, P.J. Conlon, K.L. Lynn, M.K. Farrington, T. Creazzo, A.F. Hawkins, N.

Daskalakis, S.Y. Kwan, S. Ebersviller, J.L. Burchette, M.A. Pericak-Vance, D.N. Howell, J.M. Vance, and P.B. Rosenberg, A mutation in the TRPC6 cation channel causes familial focal segmental glomerulosclerosis. Science 308 (2005) 1801-4.

[57] C.C. Moller, C. Wei, M.M. Altintas, J. Li, A. Greka, T. Ohse, J.W. Pippin, M.P. Rastaldi, S. Wawersik, S. Schiavi, A. Henger, M. Kretzler, S.J. Shankland, and J. Reiser, Induction of TRPC6 channel in acquired forms of proteinuric kidney disease. J Am Soc Nephrol 18 (2007) 29-36.

[58] R. Sonneveld, J. van der Vlag, M.P. Baltissen, S.A. Verkaart, J.F. Wetzels, J.H. Berden, J.G. Hoenderop, and T. Nijenhuis, Glucose specifically regulates TRPC6 expression in the podocyte in an AngII-dependent manner. Am J Pathol 184 (2014) 1715-26.

[59] D.V. Ilatovskaya, V. Levchenko, A. Lowing, L.S. Shuyskiy, O. Palygin, and A. Staruschenko, Podocyte injury in diabetic nephropathy: implications of angiotensin II-dependent activation of TRPC channels. Sci Rep 5 (2015) 17637.

[60] X.M. Yao, Y.J. Liu, Y.M. Wang, H. Wang, B.B. Zhu, Y.P. Liang, W.G. Yao, H. Yu, N.S. Wang, X.M. Zhang, and W. Peng, Astragaloside IV prevents high glucose-induced podocyte apoptosis via downregulation of TRPC6. Mol Med Rep 13 (2016) 5149-56.

[61] J. Reiser, K.R. Polu, C.C. Moller, P. Kenlan, M.M. Altintas, C. Wei, C. Faul, S. Herbert, I. Villegas, C. Avila-Casado, M. McGee, H. Sugimoto, D. Brown, R. Kalluri, P. Mundel, P.L. Smith, D.E. Clapham, and M.R. Pollak, TRPC6 is a glomerular slit diaphragm-associated channel required for normal renal function. Nat Genet 37 (2005) 739-44.

[62] A.D. Kistler, G. Singh, M.M. Altintas, H. Yu, I.C. Fernandez, C. Gu, C. Wilson, S.K. Srivastava, A. Dietrich, K. Walz, D. Kerjaschki, P. Ruiz, S. Dryer, S. Sever, A.K. Dinda, C. Faul, and J. Reiser, Transient receptor potential channel 6 (TRPC6) protects podocytes during complement-mediated glomerular disease. J Biol Chem 288 (2013) 36598-609.

[63] J.M. Hofstra, M.J. Coenen, M.M. Schijvenaars, J.H. Berden, J. van der Vlag, L.H. Hoefsloot, N.V. Knoers, J.F. Wetzels, and T. Nijenhuis, TRPC6 single nucleotide polymorphisms and progression of idiopathic membranous nephropathy. PLoS One 9 (2014) e102065.

[64] K. Smedlund, and G. Vazquez, Involvement of native TRPC3 proteins in ATP-dependent expression of VCAM-1 and monocyte adherence in coronary artery

endothelial cells. Arterioscler Thromb Vasc Biol 28 (2008) 2049-55.

[65] F. Thilo, A. Scholze, D.Y. Liu, W. Zidek, and M. Tepel, Association of transient receptor potential canonical type 3 (TRPC3) channel transcripts with proinflammatory cytokines. Arch Biochem Biophys 471 (2008) 57-62.

[66] K. Smedlund, J.Y. Tano, and G. Vazquez, The constitutive function of native TRPC3 channels modulates vascular cell adhesion molecule-1 expression in coronary endothelial cells through nuclear factor kappaB signaling. Circ Res 106 (2010) 1479-88.

[67] K.B. Smedlund, L. Birnbaumer, and G. Vazquez, Increased size and cellularity of advanced atherosclerotic lesions in mice with endothelial overexpression of the human TRPC3 channel. Proc Natl Acad Sci U S A 112 (2015) E2201-6.

[68] M. Riehle, A.K. Buscher, B.O. Gohlke, M. Kassmann, M. Kolatsi-Joannou, J.H. Brasen, M. Nagel, J.U. Becker, P. Winyard, P.F. Hoyer, R. Preissner, D. Krautwurst, M. Gollasch, S. Weber, and C. Harteneck, TRPC6 G757D Loss-of-Function Mutation Associates with FSGS. J Am Soc Nephrol 27 (2016) 2771-83.

[69] N. Urban, L. Wang, S. Kwiek, J. Rademann, W.M. Kuebler, and M. Schaefer, Identification and Validation of Larixyl Acetate as a Potent TRPC6 Inhibitor. Mol Pharmacol 89 (2016) 197-213.

[70] N. Urban, S. Neuser, A. Hentschel, S. Kohling, J. Rademann, and M. Schaefer, Pharmacological inhibition of focal segmental glomerulosclerosis-related, gain of function mutants of TRPC6 channels by semi-synthetic derivatives of larixol. Br J Pharmacol 174 (2017) 4099-4122.

[71] S. Hafner, F. Burg, M. Kannler, N. Urban, P. Mayer, A. Dietrich, D. Trauner, J. Broichhagen, and M. Schaefer, A (+)-Larixol Congener with High Affinity and Subtype Selectivity toward TRPC6. ChemMedChem 13 (2018) 1028-1035.

[72] B. Liu, X. He, S. Li, B. Xu, L. Birnbaumer, and Y. Liao, Deletion of diacylglycerol-responsive TRPC genes attenuates diabetic nephropathy by inhibiting activation of the TGFbeta1 signaling pathway. Am J Transl Res 9 (2017) 5619-5630.

[73] J. van der Wijst, and R.J.M. Bindels, Renal physiology: TRPC5 inhibition to treat progressive kidney disease. Nat Rev Nephrol 14 (2018) 145-146.

[74] X. Wang, R.R. Dande, H. Yu, B. Samelko, R.E. Miller, M.M. Altintas, and J. Reiser, TRPC5 Does Not Cause or Aggravate Glomerular Disease. J Am Soc Nephrol 29 (2018) 409-415.

[75] D.R. Wilson, Renal function during and following obstruction. Annu Rev Med 28 (1977)

329-39.

[76] C.C. Capelouto, and B. Saltzman, The pathophysiology of ureteral obstruction. J Endourol 7 (1993) 93-103.

[77] F. Strutz, and M. Zeisberg, Renal fibroblasts and myofibroblasts in chronic kidney disease. J Am Soc Nephrol 17 (2006) 2992-8.

[78] T. Kawakami, I. Mimura, K. Shoji, T. Tanaka, and M. Nangaku, Hypoxia and fibrosis in chronic kidney disease: crossing at pericytes. Kidney Int Suppl (2011) 4 (2014) 107-112.

[79] J. Davis, A.R. Burr, G.F. Davis, L. Birnbaumer, and J.D. Molkentin, A TRPC6-dependent pathway for myofibroblast transdifferentiation and wound healing in vivo. Dev Cell 23 (2012) 705-15.

[80] K. Hofmann, S. Fiedler, S. Vierkotten, J. Weber, S. Klee, J. Jia, W. Zwickenpflug, V. Flockerzi, U. Storch, A.O. Yildirim, T. Gudermann, M. Konigshoff, and A. Dietrich, Classical transient receptor potential 6 (TRPC6) channels support myofibroblast differentiation and development of experimental pulmonary fibrosis. Biochim Biophys Acta 1863 (2017) 560-568.

[81] J. Baum, and H.S. Duffy, Fibroblasts and myofibroblasts: what are we talking about? J Cardiovasc Pharmacol 57 (2011) 376-9.

[82] M.J. Berridge, Calcium signalling remodelling and disease. Biochem Soc Trans 40 (2012) 297-309.

[83] C. Kurts, U. Panzer, H.J. Anders, and A.J. Rees, The immune system and kidney disease: basic concepts and clinical implications. Nat Rev Immunol 13 (2013) 738-53.

[84] R.B. Mannon, A.J. Matas, J. Grande, R. Leduc, J. Connett, B. Kasiske, J.M. Cecka, R.S. Gaston, F. Cosio, S. Gourishankar, P.F. Halloran, L. Hunsicker, D. Rush, and K.A.F.I. De, Inflammation in areas of tubular atrophy in kidney allograft biopsies: a potent predictor of allograft failure. Am J Transplant 10 (2010) 2066-73.

[85] K.I. Swenson-Fields, C.J. Vivian, S.M. Salah, J.D. Peda, B.M. Davis, N. van Rooijen, D.P. Wallace, and T.A. Fields, Macrophages promote polycystic kidney disease progression. Kidney Int 83 (2013) 855-64.

[86] B. Yadav, N. Prasad, V. Agrawal, M. Jain, V. Agarwal, A. Jaiswal, D. Bhadauria, R.K. Sharma, and A. Gupta, T-bet-positive mononuclear cell infiltration is associated with transplant glomerulopathy and interstitial fibrosis and tubular atrophy in renal allograft recipients. Exp Clin Transplant 13 (2015) 145-51.

[87] S.K. Park, M.J. Kang, W. Kim, and G.Y. Koh, Renal tubule regeneration after ischemic injury is coupled to the up-regulation and activation of cyclins and cyclin dependent kinases. Kidney Int 52 (1997) 706-14.

[88] S. Qi, and D. Wu, Bone marrow-derived mesenchymal stem cells protect against cisplatin-induced acute kidney injury in rats by inhibiting cell apoptosis. Int J Mol Med 32 (2013) 1262-72.

[89] K. Berger, and M.J. Moeller, Mechanisms of epithelial repair and regeneration after acute kidney injury. Semin Nephrol 34 (2014) 394-403.

[90] I. Hirschler-Laszkiewicz, Q. Tong, K. Conrad, W. Zhang, W.W. Flint, A.J. Barber, D.L. Barber, J.Y. Cheung, and B.A. Miller, TRPC3 activation by erythropoietin is modulated by TRPC6. J Biol Chem 284 (2009) 4567-81.

[91] B.C. Liu, X. Song, X.Y. Lu, D.T. Li, D.C. Eaton, B.Z. Shen, X.Q. Li, and H.P. Ma, High glucose induces podocyte apoptosis by stimulating TRPC6 via elevation of reactive oxygen species. Biochim Biophys Acta 1833 (2013) 1434-42.

[92] Y. Zhang, W. Qin, L. Zhang, X. Wu, N. Du, Y. Hu, X. Li, N. Shen, D. Xiao, H. Zhang, Z. Li, Y. Zhang, H. Yang, F. Gao, Z. Du, C. Xu, and B. Yang, MicroRNA-26a prevents endothelial cell apoptosis by directly targeting TRPC6 in the setting of atherosclerosis. Sci Rep 5 (2015) 9401.

[93] F.J. Kubben, A. Peeters-Haesevoets, L.G. Engels, C.G. Baeten, B. Schutte, J.W. Arends, R.W. Stockbrugger, and G.H. Blijham, Proliferating cell nuclear antigen (PCNA): a new marker to study human colonic cell proliferation. Gut 35 (1994) 530-5.

[94] Z. Saifudeen, J. Marks, H. Du, and S.S. El-Dahr, Spatial repression of PCNA by p53 during kidney development. Am J Physiol Renal Physiol 283 (2002) F727-33.

[95] P. Perucca, S. Sommatis, R. Mocchi, E. Prosperi, L.A. Stivala, and O. Cazzalini, A DDB2 mutant protein unable to interact with PCNA promotes cell cycle progression of human transformed embryonic kidney cells. Cell Cycle 14 (2015) 3920-8.

[96] C.E. Koro, B.H. Lee, and S.J. Bowlin, Antidiabetic medication use and prevalence of chronic kidney disease among patients with type 2 diabetes mellitus in the United States. Clin Ther 31 (2009) 2608-17.

[97] D. Lizicarova, B. Krahulec, E. Hirnerova, L. Gaspar, and Z. Celecova, Risk factors in diabetic nephropathy progression at present. Bratisl Lek Listy 115 (2014) 517-21.

[98] J. Eckel, P.J. Lavin, E.A. Finch, N. Mukerji, J. Burch, R. Gbadegesin, G. Wu, B. Bowling, A. Byrd, G. Hall, M. Sparks, Z.S. Zhang, A. Homstad, L. Barisoni, L.

Birbaumer, P. Rosenberg, and M.P. Winn, TRPC6 enhances angiotensin II-induced albuminuria. J Am Soc Nephrol 22 (2011) 526-35.

[99] J.H. Kim, J. Xie, K.H. Hwang, Y.L. Wu, N. Oliver, M. Eom, K.S. Park, N. Barrezueta, I.D. Kong, R.P. Fracasso, C.L. Huang, and S.K. Cha, Klotho May Ameliorate Proteinuria by Targeting TRPC6 Channels in Podocytes. J Am Soc Nephrol 28 (2017) 140-151.

Chapter 7
Appendix / Anhang

7.1 Declaration of candidate / Eidesstattliche Versicherung

„Ich, Weiying Kong, versichere an Eides statt durch meine eigenhändige Unterschrift, dass ich die vorgelegte Dissertation mit dem Thema: „TRPC6 in Renal Fibrosis and Immune Cell Infiltration after Unilateral Ureteral Obstruction“ selbstständig und ohne nicht offengelegte Hilfe Dritter verfasst und keine anderen als die angegebenen Quellen und Hilfsmittel genutzt habe.

Alle Stellen, die wörtlich oder dem Sinne nach auf Publikationen oder Vorträgen anderer Autoren beruhen, sind als solche in korrekter Zitierung (siehe „Uniform Requirements for Manuscripts (URM)“ des ICMJE -*www.**icmje**.org*) kenntlich gemacht. Die Abschnitte zu Methodik (insbesondere praktische Arbeiten, Laborbestimmungen, statistische Aufarbeitung) und Resultaten (insbesondere Abbildungen, Graphiken und Tabellen) entsprechen den URM (s.o) und werden von mir verantwortet.

Meine Anteile an etwaigen Publikationen zu dieser Dissertation entsprechen denen, die in der untenstehenden gemeinsamen Erklärung mit dem/der Betreuer/in, angegeben sind. Sämtliche Publikationen, die aus dieser Dissertation hervorgegangen sind und bei denen ich Autor bin, entsprechen den URM (s.o) und werden von mir verantwortet.

Die Bedeutung dieser eidesstattlichen Versicherung und die strafrechtlichen Folgen einer unwahren eidesstattlichen Versicherung (§156,161 des Strafgesetzbuches) sind mir bekannt und bewusst.“

Datum 20.11.2018 Unterschrift

7.2 Curriculum vitae / Lebenslauf

Mein Lebenslauf wird aus datenschutzrechtlichen Gründen in der elektronischen Version meiner Arbeit nicht veröffentlicht.

Mein Lebenslauf wird aus datenschutzrechtlichen Gründen in der elektronischen Version meiner Arbeit nicht veröffentlicht.

7.3 List of publications / Publikationsliste

Kong W, Haschler TN, Nürnberg B, Krämer S, Gollasch M, Markó L. Renal Fibrosis, Immune Cell Infiltration and Changes of TRPC Channel Expression after Unilateral Ureteral Obstruction in *Trpc6*$^{-/-}$ Mice. *Cellular Physiology and Biochemistry, 2019;52(6):1484-1502. doi: 10.33594/000000103.*

7.4 Acknowledgements / Danksagung

An erster Stelle danke ich meinem Doktorvater, Herrn Prof. Dr. Dr. Maik Gollasch, für seine umfassende Betreuung und Unterstützung. Dank seiner herausragenden Expertise konnte er mich immer wieder bei meinen Fragen unterstützen. Er war nahezu jederzeit für uns erreichbar, um die neuen Probleme und Ideen der Arbeit zu besprechen. Vielen Dank für die Zeit und Mühen!

Frau Prof. Dr. Stephanie Krämer danke ich für die Möglichkeit, die Tierversuche im Deutschen Institut für Ernährungsforschung (DIfE) durchzuführen. Ich bin sehr dankbar dafür, dass sie mir alle chirurgischen Kenntnisse und Fähigkeiten für den Tierversuch beigebracht hat.

Ich möchte mich auch bei allen Mitarbeitern des Max-Rubner-Labors im DIfE bedanken, insbesondere Frau Alice Mika und Frau Dr. Tina Nitezki für die ausführliche Einweisung in die Laborarbeit und den Tierversuch. Mein besonderer Dank geht an Frau Elisabeth Meyer für die Hilfe bei den immunhistochemischen Färbungen und die freundliche Einweisung in die technischen Details des Färbeprozesses. Herrn Timo Nicolas Haschler danke ich für seine Vorarbeit (Abbildungen 3.2B, 3.3B,D, 3.4B,D und 3.6) und wertvolle Erfahrungen.

Bei Herrn Dr. Lajos Markó bedanke ich mich für seine kompetente und geduldige Hilfe bei den qPCR Versuchen und der Ergebnisauswertung. Ohne ihn hätte ich die Arbeit nicht erfolgreich anfertigen können. Mein Dank gilt auch den technischen Mitarbeiterinnen der AG Müller/Dechend, Frau Jana Czychi, Frau Juliane Anders und Frau Gabriele N'diaye, hier für die freundliche Unterstützung bei der Anleitung in den experimentellen Techniken.

Ganz besonders herzlich bedanke ich mich bei Herrn Prof. Dr. Dr. Bernd Nürnberg für die großzügige Unterstützung beim Verfassen meiner Arbeit.

Allen Mitgliedern der AG Gollasch möchte ich für ihre Unterstützung und angenehme Zusammenarbeit während meiner Arbeit danken. Herrn Dr. Mario Kaßmann, Frau

Kornelia Buttke und Herrn Dr. Dmitry Tsvetkov danke ich in besonderer Weise für die Einführung in die Laborarbeit und die experimentellen Grundlagen zur Durchführung der Versuche. Weiterhin gilt mein Dank Frau Yoland-Marie Anistan, Frau Ning Wang, Frau Xiaoming Lian, Herrn Gang Fan und Frau Nadine Wittstruck für die kollegiale Atmosphäre im Labor.

Meinen Freunden danke ich für die Freundschaft und geistige Unterstützung ungeachtet der geographischen Distanzen, die das Leben mit sich bringt. Insbesondere bedanke ich mich bei Frau Ying Zhou für die statistische Hilfe und Beratung.

Nicht zuletzt danke ich meinen Eltern, dass sie mir über lange Zeit des Studiums immer mit Rat und Tat zur Seite standen und mich ohne Zögern unterstützt haben. Ich liebe euch!

Ich kann nicht in Worten ausdrücken, wie dankbar ich bin. Einfach, Dankeschön an alle für alles!